

Synthesis of semiconductor nanocrystals in organic solvents

By

Peter Reiss

CEA Grenoble DSM/INAC/SPrAM (UMR 5819 CEA-CNRS-Université Joseph Fourier),
Laboratoire d'Electronique Moléculaire, Organique et Hybride, Grenoble, France

1. Introduction

Colloidal semiconductor nanocrystals (NCs) are crystalline particles with diameters ranging typically from 1 to 10 nm, comprising some hundreds to a few thousands of atoms. The inorganic core consisting of the semiconductor material is capped by an organic outer layer of surfactant molecules (“ligands”), which provide sufficient repulsion between the crystals to prevent them from agglomeration. In the nanometer size regime many physical properties of the semiconductor particles change with respect to the bulk material. Examples of this behavior are melting points and charging energies of NCs, which are, to a first approximation, proportional to the reciprocal value of their radii. At the origin of the great interest in NCs was yet another observation, namely the possibility of changing the semiconductor band gap – that is the energy difference between the electron-filled valence band and the empty conduction band – by varying the particle size. In a bulk semiconductor an electron e^- can be excited from the valence to the conduction band by absorption of a photon with an appropriate energy, leaving a hole h^+ in the valence band. Feeling each other’s charge, the electron and hole do not move independently from each other because of the Coulomb attraction. The formed e^-h^+ bound pair is called an exciton and has its lowest energy state slightly below the lower edge of the conduction band. At the same time its wave function is extended over a large region (several lattice spacings), i.e. the exciton radius is large, since the effective masses of the charge carriers are small and the dielectric constant is high [1]. To give examples, the Bohr exciton radii in bulk CdS and CdSe are approximately 3 and 5 nm. Reduction of the particle size to a few nanometers produces the unusual situation that the exciton size can exceed the crystal dimensions. To “fit” into the NC, the charge carriers have to assume higher kinetic energies leading to an increasing band gap and quantization of the energy levels to discrete values. This phenomenon is commonly called “*quantum confinement effect*” [2], and its theoretical treatment is usually based on the quantum mechanical particle-in-a-box model [3]. With decreasing particle size, the energetic structure of the NCs (also termed *quantum dots*) changes from a band-like one to discrete levels. Therefore, in some cases a description by means of molecular orbital theory may be more appropriate, applying

the terms HOMO (highest occupied molecular orbital) and LUMO (lowest unoccupied molecular orbital) instead of conduction band and valence band. This ambiguity in terminology reflects the fact that the properties of semiconductor NCs lie in between those of the corresponding bulk material and molecular compounds. The unique optical properties of semiconductor NCs are exploited in a large variety of applications essentially in the fields of biological labeling and (opto-)electronics.

Initiated by pioneering work in the early 1980s [4–7], the research on semiconductor NCs went through a remarkable progress after the development of a novel chemical synthesis method in 1993, which allowed for the preparation of samples with a low size dispersion [8]. The physical properties of NCs, and in particular the optical ones, are strongly size-dependent. To give an example, the linewidth of the photoluminescence (PL) peak is directly related to the size dispersion of the NCs, and thus a narrow size distribution is necessary to obtain a pure emission colour. It is common practice to term samples whose deviation from the mean size is inferior or equal to 5–10% as “monodisperse”. The method developed by Murray et al. [8] was the first one to allow for the synthesis of monodisperse cadmium chalcogenide NCs in a size range of 2–12 nm. It relies on the rapid injection of organometallic precursors into a hot organic solvent. Numerous synthesis methods deriving from the original one have been reported in literature in the last 15 years. Nowadays a much better understanding of the influence of the different reaction parameters has been achieved, allowing for the rational design of synthesis protocols.

The goal of this chapter is to give a representative overview of the state of the art concerning the chemical synthesis of semiconductor NCs/quantum dots in organic solvents with a special emphasis on recent developments. Surface functionalization as well as applications of semiconductor NCs go beyond the scope of this chapter. Several reviews on NCs' synthesis have appeared in the literature during the last 5 years [9–12]. In addition, the synthesis of core/shell (CS) structures, comprising a NC of a first semiconductor (*core*), surrounded by an epitaxial, generally 0.5–2-nm thick layer of another semiconductor (*shell*) is discussed. Core/shell systems are intensively studied due to their superior optical properties and higher stability as compared to core NCs. On the other hand, differing synthesis methods, such as the preparation of NCs in aqueous media [13, 14], in microemulsions [15], at the oil-water interface [16], in ionic liquids [17] or in supercritical fluids [18] are not treated here. Concerning the shape control of NCs, the preparation of core/multishell structures, or the synthesis of NCs or heterostructures comprising other types of materials than semiconductors (e.g. oxides or metals), the interested reader is referred to other chapters of this book.

The text is organized as follows:

Succeeding this introduction (Sect. 1), a brief description of the basic optical and structural properties of semiconductor NCs is given (Sect. 2). In addition, the general principles of the synthesis of core and core/shell NCs in organic solvents at elevated temperature are outlined.

In Sect. 3, the current state of the art concerning the synthesis of core NCs of different families of elemental and compound (binary and tertiary) semiconductors is reviewed. Section 4 deals with the preparation of core/shell structures comprising two different semiconductors. At the same time, the consequences of the band

alignment, i.e. the relative positions of the electronic energy levels of both constituents, on the optical properties of the NCs are discussed. Finally, it is attempted to sketch some perspectives concerning the development of this domain in the near future (Sect. 5).

2. Basic properties of nanocrystals

2.1 Optical properties of semiconductor nanocrystals

2.1.1 Absorption. As it has already been stated in the introduction, absorption of a photon by the NC occurs if its energy exceeds the band gap. Due to quantum confinement, decreasing the particle size results in a hypsochromic (blue-) shift of the absorption onset [19]. A relatively sharp absorption feature near the absorption onset corresponds to the excitonic peak, i.e. the lowest excited state exhibiting a large oscillator strength (cf. Fig. 1). While its position depends on the band gap and, consequently, on the particle size, its form and width is strongly influenced by the

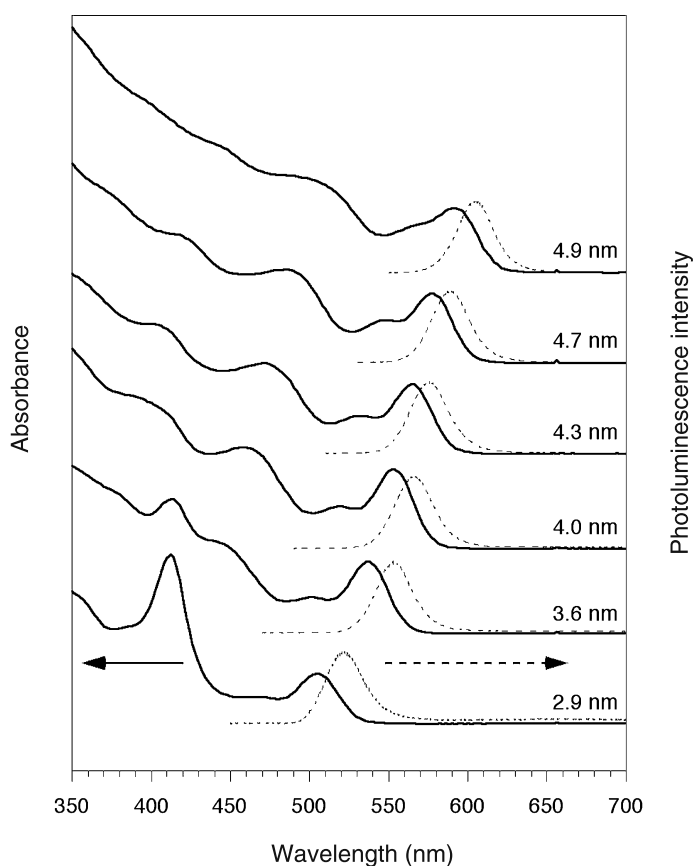


Fig. 1. Absorption and normalized photoluminescence spectra of a size series of CdSe NCs (spectra vertically shifted for clarity) [21]

distribution in size, as well as the form and stoichiometry of the NCs. Therefore polydisperse samples typically exhibit only a shoulder in the absorption spectrum at the position of the excitonic transition. Less pronounced absorption features in the shorter wavelength range correspond to excited states of higher energy [20]. As a rule of thumb, it can be asserted that the larger the number of such spectral features and the more distinctly they are resolved in the absorption spectrum, the smaller is the size dispersion of the sample. In Fig. 1 the absorption and photoluminescence spectra of a series of CdSe NCs differing in size are depicted.

2.1.2 Photoluminescence. Photoluminescence, i.e. the generation of luminescence through excitation by photons, is formally divided into two categories, fluorescence and phosphorescence, depending upon the electronic configuration of the excited state and the emission pathway. Fluorescence is the property of a semiconductor to absorb photons with an energy $h\nu_e$ superior to its band gap, and – after charge carrier relaxation via phonons to the lowest excited state – to emit light of a higher wavelength (lower energy $h\nu_f$) after a brief interval, called the fluorescence lifetime (Fig. 2). The process of phosphorescence occurs in a similar manner, but with a much longer excited state lifetime, due to the symmetry of the state.

The emitted photons have an energy corresponding to the band gap of the NCs and for this reason the emission colour can be tuned by changing the particle size. It should be noted here that efficient room temperature band edge emission is only observed for NCs with proper surface passivation because otherwise charge carriers are very likely to be trapped in surface states, enhancing non-radiative recombination. Due to spectral diffusion and the size distribution of NCs, the room temperature luminescence linewidths of ensembles lie for the best samples of CdSe NCs in the range of 20–25 nm (full width at half maximum, FWHM). As can be seen in Fig. 1, the maxima of the emission peak are red-shifted by ca. 10–20 nm as compared to the excitonic peak in the absorption spectra. This phenomenon is usually referred to as Stokes-shift and has its origin in the particular structure of the exciton energy levels inside the NC. Models using the effective mass approximation show that in bulk wurtzite CdSe the exciton state ($1S_{3/2}1S_e$) is eight-fold degenerate [22]. In CdSe NCs,

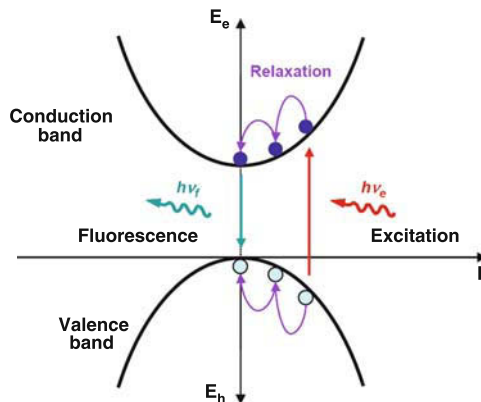


Fig. 2. Fluorescence in a bulk semiconductor

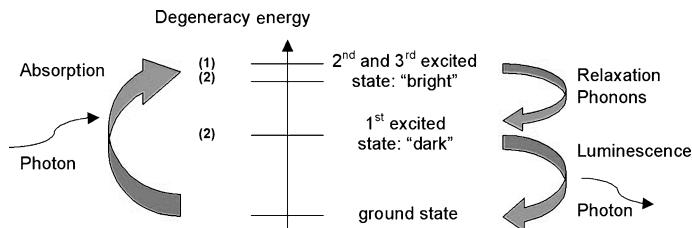


Fig. 3. Schematic representation of the exciton states of CdSe NCs involved in absorption and emission processes

this degeneracy is partially lifted and the band edge state is split into five states, due to the influence of the internal crystal field, effects arising from the non-spherical particle shape and the electron–hole exchange interaction (see Fig. 3). The latter term is strongly enhanced by quantum confinement [23].

Two states, one singlet state and one doublet state, are optically inactive for symmetry reasons. The energetic order of the three remaining states depends on the size and form of the NC. In the case of weak excitation on a given state, absorption depends exclusively on its oscillator strength. As the oscillator strength of the second and third excited (“bright”) states is significantly higher than that of the first (“dark”) one, excitation by photon absorption occurs to the bright states. On the opposite, photoluminescence depends on the product of oscillator strength and population of the concerned state. Relaxation via acoustic phonon emission from bright states to the dark band edge state causes strong population of the latter and enables radiative recombination (Fig. 3). This model is corroborated by the experimental room temperature values of the Stokes-shift, which are consistent with the energy differences between the related bright and dark states.

2.1.3 Emission of single nanocrystals, blinking phenomenon. Spectroscopic investigation of single semiconductor NCs revealed that their emission under continuous excitation turns on and off intermittently. This blinking is a common feature also for other nanostructured materials, involving porous Si [24] and epitaxially grown InP quantum dots [25], as well as chromophores at the single molecule level such as polymer segments [26], organic dye molecules [27] and green fluorescent protein (GFP) [28]. However, the origin of the intermittence is completely different for NCs and single dye molecules: in the latter resonant excitation into a single absorbing state takes place. Due to spectral shifting events the excitation is no longer in resonance and a dark period begins. NCs, on the other hand, are excited non-resonantly into a large density of states above the band edge. While their emission statistics and its modelling is the issue of a large number of publications, detailed understanding of the blinking phenomenon has not yet been achieved. The sequence of “on” and “off” periods resembles a random telegraph signal on a time scale varying over several orders of magnitude up to minutes and follows a temporal statistics described by an inverse power law [29]. Transition from an “on” to an “off” state of the NC occurs by photo-ionization, which implies the trapping of a charge carrier in the surrounding matrix (dangling bonds on the surface, solvent, etc.). A single delocalized electron or hole rests in the NC core. Upon further excitation this

gives rise to fast (nanosecond order) non-radiative relaxation through Auger processes, i.e. energy transfer from the created exciton to the delocalized charge carrier [30]. Mechanisms for a return to the “on” state are the recapture of the localized charge carrier into the core or the capture of an opposite charge carrier from traps in the proximity. Both pathways can be accompanied by a reorganization of the charge distribution around the NCs. As a consequence the local electric field changes leading to a Stark shift of the photoluminescence peak [31, 32].

2.1.4 Efficiency of the emission: fluorescence quantum yield. The emission efficiency of an ensemble of NCs is expressed in terms of the fluorescence quantum yield (Q.Y.), i.e. the ratio between the number of absorbed photons and the number of emitted photons. As a consequence of the blinking phenomenon (*vide supra*) the theoretical value of 1 is hard to observe because a certain number of NCs are in “off” states. Furthermore the Q.Y. may be additionally reduced as a result of quenching caused by surface trap states. As both of these limiting factors are closely related to the quality of the NC surface, they can be considerably diminished by its improved passivation. This can be achieved by changing the nature of the organic ligands, capping the NCs after their synthesis. To give an example, after substitution of the trioctylphosphine oxide (TOPO) cap on CdSe NCs by hexadecylamine (HDA) or allylamine, an increase of the Q.Y. from about 10% to values of 40–50% has been reported [33]. In this case better surface passivation probably results from an increased capping density of the sterically less-hindered amines as compared to TOPO. Very recently the influence of thiol and amine ligands on the PL properties of CdSe-based NCs has been studied in further details by Munro et al. [34]. Jang et al. obtained cadmium chalcogenide NCs with Q.Y.s up to 75% after treatment with NaBH_4 and explained the better surface passivation by the formation of a cadmium oxide layer [35]. In the case of III–V semiconductors, Mićić et al. and Talapin et al. reported an enhancement of the PL Q.Y. of InP NCs from less than 1% to 25–40% upon treatment with HF [36, 37]. Here the improved emission properties have been attributed to the removal of phosphorus dangling bonds under PF_3 elimination from the NC surface.

However, in view of further NC functionalization, it is highly desirable to provide a surface passivation, which is insensitive to subsequent ligand exchange. This is obviously not the case with the described procedures for Q.Y. enhancement. A suitable and widely applied method consists of the growth of an inorganic shell on the surface of the NCs. The resulting core/shell systems will be described in detail in Sect. 2.3.

2.2 Structural properties of nanocrystals. Most binary octet semiconductors crystallize either in the cubic zinc blende (ZB) or in the hexagonal wurtzite (W) structure, both of which are four-coordinate and vary in the layer stacking along (111), showing an ABCABC or an ABAB sequence, respectively (Fig. 4).

The room temperature ground state structures of selected II–VI, III–V and IV–VI semiconductors are given in Table 1 (Sect. 2.4.1). In cases of relatively low difference in the total energy between the ZB and the W structure (e.g. CdTe, ZnSe), the materials exhibit the so-called W–ZB polytypism [38]. Depending on the

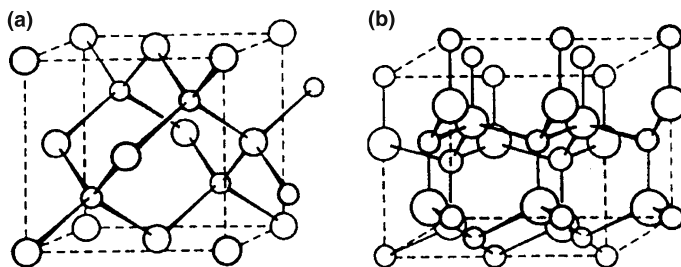
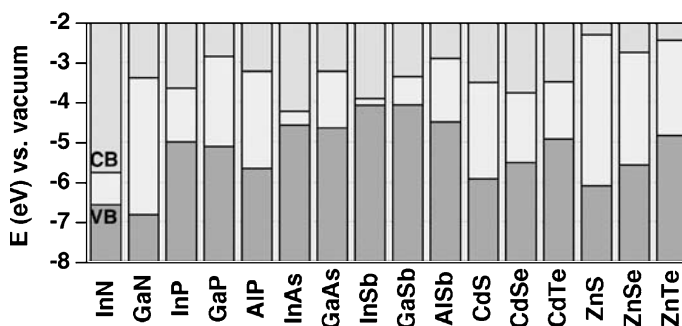


Fig. 4. **a** Zinc blende, **b** wurtzite crystal structure

experimental conditions, nucleation and growth of the NCs can take place in either structure and also the coexistence of both structures in the same nanoparticle is possible. Lead chalcogenide NCs crystallize in the six-coordinate rocksalt structure (cf. Table 1, p 46), and it has been shown that also CdSe NCs can exist in this crystal structure at ambient pressure, provided that their diameter exceeds a threshold size of 11 nm, below which they transform back to the four-coordinate structure [39].

2.3 Core/shell structures. Surface engineering is an important tool to control the properties of the NCs and in particular the optical ones. One important strategy is the overgrowth of NCs with a shell of a second semiconductor, resulting in CS systems. This method has been applied to improve the fluorescence Q.Y. and the stability against photo-oxidation but also, by proper choice of the core and shell materials, to tune the emission wavelength in a large spectral window. After pioneering work in the 1980s and the development of powerful chemical synthesis routes in the end of the 1990s [40–42], a strongly increasing number of articles have been devoted to CS NCs in the last 5 years. Nowadays, almost any type of core NC prepared by a robust chemical synthesis method has been overgrown with shells of other semiconductor materials.

Depending on the band gaps and the relative position of electronic energy levels of the involved semiconductors, the shell can have different functions in CS NCs.



Scheme 1. Electronic energy levels of selected III-V and II-VI semiconductors using the valence band offsets from [43] (VB: valence band, CB: conduction band)

Scheme 1 gives an overview of the band alignment of the bulk materials, which are mostly used in NC synthesis. Two main cases can be distinguished, denominated type I and type II band alignment, respectively. In the former, the band gap of the shell material is larger than that of the core one, and both electrons and holes are confined in the core. In the latter, either the valence band edge or the conduction band edge of the shell material is located in the band gap of the core. The resulting staggered band alignment leads upon excitation of the NC to a spatial separation of the hole and the electron in different regions of the CS structure.

At this point, it is important to stress that the type I/type II distinction must not be mistaken for the difference between direct and indirect semiconductors. In the first case, type I heterostructures experience optical transitions between electron and hole states, whose wavefunctions are localized in the same region in the *real space*, whereas for type II heterostructures, the electron and hole lie in different regions (here, the core and shell of the NCs). In the second case, the distinction between direct and indirect semiconductors concerns transitions between electron and hole states located at the same (direct) or at different (indirect) points in the *reciprocal (wavevector) space*. Indirect optical transitions involve the simultaneous emission or absorption of a phonon, thus having a much lower probability than direct transitions. A typical example of an indirect semiconductor is silicon, consequently exhibiting a very low fluorescence Q.Y. in its bulk form.

In type I CS NCs, the shell is used to “passivate” the surface of the core with the goal to improve its optical properties. The shell separates physically the surface of the optically active core NC from its surrounding medium. As a consequence, the sensitivity of the optical properties to changes in the local environment of the NCs’ surface, induced for example by the presence of oxygen or water molecules, is reduced. With respect to core NCs, CS systems exhibit generally enhanced stability against photo-degradation. At the same time, shell growth reduces the number of surface dangling bonds, which can act as trap states for charge carriers and reduce the fluorescence Q.Y. The first published prototype system was CdSe/ZnS [40]. The ZnS shell significantly improves the fluorescence Q.Y. and stability against photo-bleaching. Shell growth is accompanied by a *small* red shift (5–10 nm) of the excitonic peak in the UV–vis absorption spectrum and the PL wavelength. This observation is attributed to a partial leakage of the exciton into the shell material.

In type II systems, shell growth aims at a *significant* red shift of the emission wavelength of the NCs. The staggered band alignment leads to a smaller effective band gap than each one of the constituting core and shell materials. The interest of these systems is the possibility to tune the emission colour with the shell thickness towards spectral ranges, which are difficult to attain with other materials. Type II NCs have been developed in particular for near infrared emission, using for example CdTe/CdSe or CdSe/ZnTe. In contrast to type I systems, the PL decay times are strongly prolonged in type II NCs due to the lower overlap of the electron and hole wavefunctions. As one of the charge carriers (electron or hole) is located in the shell, an overgrowth of type II CS NCs with an outer shell of an appropriate material can be used in the same way as in type I systems to improve the fluorescence Q.Y. and photo-stability.

2.4 Chemical synthesis of semiconductor nanocrystals

2.4.1 Synthesis methods. Historically the synthesis in aqueous media was the first successful preparation method of colloidal semiconductor NCs. Therefore, it is briefly described in this paragraph, even though the present chapter is dedicated to the synthesis in organic solvents. The topic is addressed in details in the Chapter of Gaponik and Rogach. Initially developed procedures comprise NC formation in homogenous aqueous solutions containing appropriate reagents and surfactant-type or polymer-type stabilizers [44, 45]. The latter bind to the NC surface and stabilize the particles by steric hinderance and/or electrostatic repulsion in the case of charged stabilizers. In parallel to this monophasic synthesis, a bi-phase technique has been developed, which is based on the arrested precipitation of NCs within inverse micelles [5, 7, 46]. Here nanometer-sized water droplets (dispersed phase) are stabilized in an organic solvent (continuous phase) by an amphiphilic surfactant. They serve as nanoreactors for the NC growth and prevent at the same time from particle agglomeration. Both methods provide relatively simple experimental approaches using standard reagents as well as room temperature reactions and were of great importance for the development of NC synthesis. Furthermore, for some materials (e.g. mercury chalcogenides) [47–49] the aqueous synthetic technique is the only successful preparation method reported today. On the other hand, the samples prepared by these synthetic routes usually exhibit size dispersions at least of the order of 15% and therefore fastidious procedures of NCs separation into “sharp” fractions have to be applied in order to obtain monodisperse samples.

The introduction of a high temperature preparation method using organic solvents in 1993 [8] constituted an important step towards the fabrication of monodisperse CdS, CdSe and CdTe NCs. As demonstrated in classical studies by LaMer and Dinegar [50], the synthesis of monodisperse colloids via homogeneous nucleation requires a temporal separation of nucleation and growth of the seeds. The LaMer plot (Fig. 5) is very useful to illustrate the separation of nucleation and growth by means of a nucleation burst.

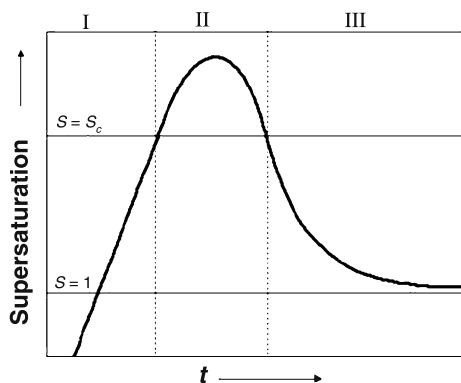


Fig. 5. LaMer plot depicting the degree of supersaturation as a function of reaction time [50]

Initially the concentration of monomers, i.e. the minimum subunits of the crystal, constantly increases by addition from exterior or by in situ generation within the reaction medium. It should be noted that in stage I no nucleation occurs even in supersaturated solution ($S > 1$), due to the extremely high energy barrier for spontaneous homogeneous nucleation. The latter is overcome in stage II for a yet higher degree of supersaturation ($S > S_c$), where nucleation and formation of stable nuclei take place. As the rate of monomer consumption induced by the nucleation and growth processes exceeds the rate of monomer supply, the monomer concentration and hence the supersaturation decreases below S_c , the level at which the nucleation rate becomes zero. In the following stage III, the particle growth continues under further monomer consumption as long as the system is in the supersaturated regime.

Experimentally, the separation of nucleation and growth can be achieved by rapid injection of the reagents into the hot solvent, which raises the precursor concentration in the reaction flask above the nucleation threshold (“*hot-injection method*”) [51]. The hot-injection leads to an instantaneous nucleation, which is quickly quenched by the fast cooling of the reaction mixture (the solution to be injected is at room temperature) and by the decreased supersaturation after the nucleation burst. Another possibility relies on attaining the degree of supersaturation necessary for homogeneous nucleation via the in situ formation of reactive species upon supply of thermal energy (“*heating-up method*”) [12]. This method is widely used in the synthesis of metallic nanoparticles, but recently an increasing number of examples of semiconductor NCs prepared by this approach can be found, as will be shown in Sect. 3. In an ideal case all crystallization nuclei are created at the same time and undergo identical growth. During the growth stage it is possible to carry out subsequent injections of precursors in order to increase the mean particle size without deterioration of the narrow size distribution as long as the concentration corresponding to the critical supersaturation S_c is not exceeded. Crystal growth from solution is in many cases followed by a second distinct growth process, which is referred to as Ostwald ripening [52, 53]. It consists of the dissolution of the smallest particles because of their high surface energy and subsequent redeposition of the dissolved matter onto the bigger ones. Thereby the total number of NCs decreases, whereas their mean size increases. As shown in early studies [54], Ostwald ripening can lead to reduced size dispersions of micron-sized colloids. In the case of nanometer-sized particles, however, Ostwald ripening generally yields size dispersions of the order of 15–20% [13], and therefore the reaction should be stopped before this stage.

From a thermodynamic point of view, if diffusion is the rate-limiting step, the size-dependent growth rate can be expressed by means of the *Gibbs–Thompson equation* (Eq. 1) [55]:

$$L(r) = L_{\text{bulk}} \exp(2\gamma V_m / rRT) \quad (1)$$

$L(r)$ and L_{bulk} are the solubilities of a NC with radius r and of the bulk solid, respectively. γ is the specific surface energy, V_m the molar volume of the solid, R the gas constant and T the temperature. The validity of Eq. (1) and the focusing of size

distributions during the diffusion-controlled NC growth have been confirmed experimentally [56, 57]. Using the hot-injection or heating-up synthesis methods, it is possible to obtain samples with 5–10% standard deviation from the mean size without post-preparative size fractionation.

One of the main disadvantages of the initially reported preparation methods lies in the fact that pyrophoric organometallic precursors were applied. Their use requires special experimental precautions and their extremely high reactivity restricts the batches to laboratory scale quantities. As a result, in recent years the development of NC high temperature synthesis focused on the replacement of these organometallic precursors by easy to handle standard reagents. To give an example, in the preparation of cadmium chalcogenide NCs, dimethylcadmium has been successfully substituted by cadmium oxide or cadmium salts of weak acids (cadmium acetate, cadmium carbonate) after complexation with long chain phosphonic or carboxylic acids [58, 59]. A further modification of the high temperature methods consisted of the appropriate selection of coordinating and non-coordinating solvents, with the goal to determine their influence on the nucleation and growth kinetics of the NCs and to fine-tune the reactivity of the precursors aiming at obtain narrow size distributions of the order of 5% [60]. More recently, studies have been undertaken by means of NMR spectroscopy, giving important insight into the chemical reactions occurring during the formation of CdSe NCs using the hot-injection method [61]. Concerning other materials, it can be concluded that the synthesis methods initially developed for CdSe NCs have been adapted to the majority of II–VI and a few III–V semiconductors in the last 5 years. The exponentially increasing number of publications proves that this research field is worldwide highly active.

2.4.2 Synthesis of core/shell systems. A general requirement for the synthesis of CS NCs with satisfactory optical properties is *epitaxial-type shell growth*. Therefore an *appropriate band alignment* is not the sole criterion for materials' choice but, in addition, the core and shell materials should *crystallize in the same structure and exhibit a small lattice mismatch*. In the opposite case, the growth of the shell results in strain and the formation of defect states at the core/shell interface or within the shell. These can act as trap states for photo-generated charge carriers and diminish the fluorescence Q.Y. [62]. Table 1 lists structural parameters of selected semiconductor materials.

Good precursors for shell growth should fulfill the criteria of high reactivity and selectivity (no side reactions). For practical reasons, and in particular if an upscaling of the reaction or industrialization of the production process is aimed, additional properties of the precursors come into play. Pyrophoric and/or highly toxic compounds require special precautions for their manipulation, especially if used in large quantities. To give an example, for the synthesis of zinc sulfide shells on various core NCs, first diethylzinc (pyrophoric) and hexamethyldisilathiane (toxic) have been proposed. Even though widely used in laboratory scale syntheses, these compounds are not very suitable for a large scale production of ZnS overcoated NCs. Further criteria, which have to be taken into account for the choice of the precursors concern the environmental risks related to the use of these compounds and eventually their

Table 1. Structural parameters of selected bulk semiconductors [63, 64]

Material	Structure (300 K)	Type	E_{gap} (eV)	Lattice parameter (Å)	Density (kg/m ³)
ZnS	Zinc blende	II–VI	3.61	5.41	4090
ZnSe	Zinc blende	II–VI	2.69	5.668	5266
ZnTe	Zinc blende	II–VI	2.39	6.104	5636
CdS	Wurtzite	II–VI	2.49	4.136/6.714	4820
CdSe	Wurtzite	II–VI	1.74	4.3/7.01	5810
CdTe	Zinc blende	II–VI	1.43	6.482	5870
GaN	Wurtzite	III–V	3.44	3.188/5.185	6095
GaP	Zinc blende	III–V	2.27 i ^a	5.45	4138
GaAs	Zinc blende	III–V	1.42	5.653	5318
GaSb	Zinc blende	III–V	0.75	6.096	5614
InN	Wurtzite	III–V	0.8	3.545/5.703	6810
InP	Zinc blende	III–V	1.35	5.869	4787
InAs	Zinc blende	III–V	0.35	6.058	5667
InSb	Zinc blende	III–V	0.23	6.479	5774
PbS	Rocksalt	IV–VI	0.41	5.936	7597
PbSe	Rocksalt	IV–VI	0.28	6.117	8260
PbTe	Rocksalt	IV–VI	0.31	6.462	8219

^a Indirect band gap

degradation products, their price and their commercial availability. As it is rather difficult to satisfy all of these factors, the development of shell synthesis methods is currently an active area of research.

The control of the shell thickness is a delicate point in the fabrication of CS NCs and deserves special attention. If the shell is too thin, the passivation of the core NCs is inefficient resulting in reduced photo-stability. In the opposite case, in turn, the optical properties of the resulting CS NCs deteriorate as, driven by the lattice mismatch of the core and shell materials, defects are created with increasing shell thickness. CS systems are generally fabricated in a two-step procedure, consisting of core NCs' synthesis, followed by a purification step, and the subsequent shell growth reaction, during which a small number of monolayers (typically 1–5) of the shell material are deposited on the cores. The temperature used for the core NC synthesis is generally higher than that used for the shell growth and the shell precursors are slowly added, for example by means of a syringe pump. The major advantages over a so-called one-pot approach without intermediate purification step is the fact that unreacted precursors or side-products can be eliminated before the shell growth. The core NCs are purified by precipitation and redispersion cycles, and finally they are redispersed in the solvent used for the shell growth. In order to calculate the required amount of shell precursors to obtain the desired shell thickness, the knowledge of the concentration of the core NCs is indispensable. In the case of cadmium chalcogenide NCs, the concentration of a colloidal solution can be determined in good approximation by means of UV–vis absorption spectroscopy thanks to tabulated relationships between the excitonic peak, the NC size and the molar extinction coefficient [65]. An advanced approach for shell growth derived from chemical bath deposition techniques and aiming at the precise control of the shell thickness, is the so-called

SILAR (successive ion layer adsorption and reaction) method [66]. It is based on the formation of one monolayer at a time by alternating the injections of cationic and anionic precursors and has firstly been applied for the synthesis of CdSe/CdS CS NCs. Monodispersity of the samples was maintained for CdS shell thicknesses up to five monolayers on 3.5 nm core CdSe NCs, as reflected by the narrow PL linewidths obtained in the range of 23–26 nm (FWHM).

3. Chemical synthesis of core nanocrystals in organic solvents

3.1 II–VI semiconductor nanocrystals. Table 2 gives an overview of the combinations of precursors, stabilizers and solvents mainly used in the synthesis of II–VI semiconductor NCs. As already stated in Sect. 2, the synthesis of NCs in organic solvents can be divided into two principal groups, the *hot-injection method* and the *heating-up method*. Due to the less restrictive experimental requirements, the latter has significant advantages if the large scale production of monodisperse NCs is aimed. Therefore, a gain of importance of this method is observed within the last years.

3.1.1 Binary systems. The pioneering work of Murray et al. [8] on the synthesis of monodisperse CdSe, CdS, CdTe NCs via the hot-injection technique experienced a number of modifications since its publication in 1993. The latter can be classified into two groups, the first one aiming at the further improvement of the particles' size and shape control, and the second one at the simplification of the experimental protocol. The addition of HDA to the TOPO/trioctylphosphine(TOP) mixed solvent proposed by Talapin et al. [33] can be counted in the first group and led to an unprecedented low size distribution of the as-prepared CdSe NCs of the order of 5%. Concerning the second group, several contributions of Peng's group in the last 7 years have to be outlined. In a first time, the replacement of the pyrophoric Cd precursor dimethylcadmium by much easier to handle compounds such as cadmium oxide, cadmium acetate or cadmium nitrate was proposed [58, 59]. The latter are transformed by phosphonic or fatty acids into reactive species prior to the injection of the Se precursor. The next step concerned the substitution of the coordinating solvent TOPO by the non-coordinating one 1-octadecene (ODE) [60]. This solvent offers a number of practical advantages (liquid at room temperature, lower price and more environmentally benign than TOPO). Moreover, the use of ODE allows for a better fine-tuning of the reactivity of the Cd precursor, as the solvent does not have the additional function of being the stabilizing ligand. Fatty acids accomplish this role and it has been demonstrated that the mean size and size dispersion depend on the length of the carbonaceous chain. While also applicable to CdSe and CdTe NCs, this approach was the first one to yield monodisperse CdS NCs without additional size sorting procedures. Very recently, the use of different alkylamines as stabilizing ligands has been studied in detail, which allowed for the decrease of the reaction temperature to 150°C, 100–200°C lower than in previously reported procedures [91]. The last ingredient of the original CdSe synthesis to be replaced was the Se precursor TOP-Se. Motivated by the fact that trialkylphosphines such as TOP or TBP

Table 2. Precursors, stabilizers and solvents used in the synthesis of various II–VI semiconductor NCs

Material	Precursors and stabilizers	Solvent(s)	Method ^a	References
CdS, CdSe, CdTe	CdMe ₂ /TOP, (TMS) ₂ Se or (TMS) ₂ S or (BDMS) ₂ Te	TOPO	HI	[8]
CdSe	CdMe ₂ /TOP, TOP-Se	TOPO, HDA	HI	[33, 67]
CdSe, CdTe	CdO, TDPA, TOP-Se or TOP-Te	TOPO	HI	[58]
CdSe	CdO or Cd(ac) ₂ or CdCO ₃ , TOP-Se, TDPA or SA or LA	TOPO	HI	[59]
CdS, CdSe	CdO, S/ODE or TBP-Se/ODE, OA	ODE	HI	[60]
CdSe	Cd(st) ₂ , TOP-Se, HH or BP	HDA, octadecane	HI	[68]
CdSe	Cd(my) ₂ , Se, OA/ODE	ODE	HU	[69]
CdSe	CdO, Se/ODE, OA	ODE	HI	[70]
CdSe	CdO, Se, OA	Olive oil	HI	[71]
CdSe	Cd(st) ₂ , TBP-Se, SA, DDA	ODE	HI	[72]
CdS	Cd(ac) ₂ , S, MA	ODE	HU	[73]
CdS, ZnS	Cd(hdx) ₂ or Cd(ex) ₂ or Cd(dx) ₂ or Zn(hdx) ₂	HDA	HU	[74, 75]
CdS, ZnS	CdCl ₂ /OAm or ZnCl ₂ /OAm/ TOPO, S/OAm	OAm	HU	[76]
CdTe	CdMe ₂ , TOP-Te	DDA	HI	[77]
CdTe	CdO, TBP-Te/ODE or TOP-Te/ODE, OA	ODE	HI	[78, 79]
CdTe	CdO, TBP-Te, ODPa	ODE	HU	[69]
ZnS	Zn(st) ₂ , S/ODE	ODE, Tetracosane	HI	[80]
ZnS	ZnEt ₂ , S	HDA/ODE	HU	[81]
ZnSe	ZnEt ₂ , TOP-Se	HDA	HI	[82]
ZnSe	Zn(st) ₂ , TOP-Se	Octadecane	HI	[83]
ZnTe	Te and ZnEt ₂ in TOP	ODA, ODE	HI	[84]
HgTe	HgBr ₂ , TOP-Te	TOPO	HI	[85]
Cd _{1-x} Zn _x Se	ZnEt ₂ /TOP, CdMe ₂ /TOP	TOPO, HDA	HI	[86, 87]
Cd _{1-x} Zn _x Se	Zn(st) ₂ , Cd(st) ₂ , TOP-Se	ODE	HI	[88]
Cd _{1-x} Zn _x S	CdO, ZnO, S/ODE, OA	ODE	HI	[89]
CdSe _{1-x} Te _x	CdO, TOP-Se, TOP-Te	TOPO, HDA	HI	[90]

^a *HI* Hot-injection method; *HU* Heating-up method

CdMe₂ dimethylcadmium; *ZnEt₂* diethylzinc; *TMS* trimethylsilyl; *(BDMS)₂Te* bis(*tert*-butyldimethylsilyl) telluride; *TDPA* tetradecylphosphonic acid; *ODPA* octadecylphosphonic acid; *SA* stearic acid; *LA* lauric acid; *OA* oleic acid; *MA* myristic acid; *ac* acetate; *my* myristate; *st* stearate; *hdx* hexadecylxanthate; *ex* ethylxanthate; *dx* decylxanthate; *TOPO* trioctylphosphine oxide; *HAD* hexadecylamine; *DDA* dodecylamine; *ODA* octadecylamine; *TOP* trioctylphosphine; *TBP* tributylphosphine; *ODE* 1-octadecene; *HH* hexadecyl hexadecanoate; *BP* benzophenone

are air- and moisture-sensitive and relatively expensive compounds, the groups of Cao and of Mulvaney proposed phosphine-free synthesis methods for CdSe NCs in 2005 [69, 70]. In the first case, elemental selenium was used as the precursor in a one-pot reaction. It becomes soluble in ODE above 190°C and starts to react with the Cd precursor cadmium myristate at higher temperatures. This procedure does not require the injection of precursors into the hot reaction medium and is therefore a typical example of the heating-up method. Remarkably, the as-prepared NCs exhibit a size distribution of the order of 5% and zinc blende crystal structure. The

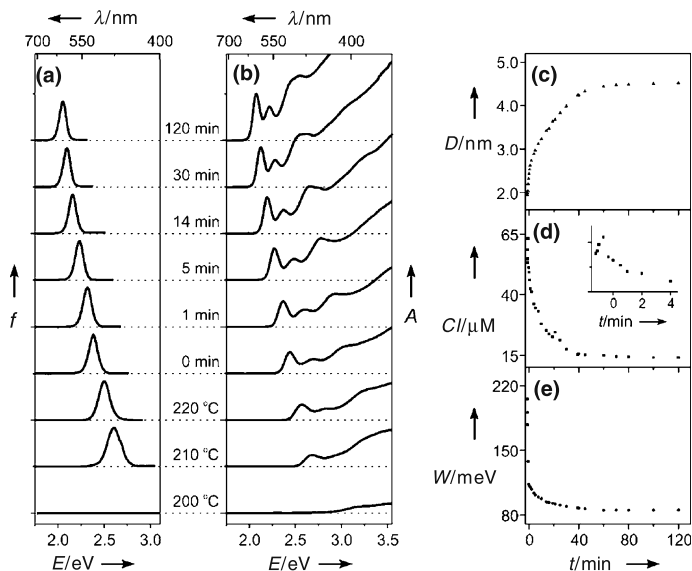


Fig. 6. Temporal evolution of **a** the fluorescence (*f*) spectrum, **b** the absorption (*A*) spectrum, **c** the diameter (*D*) of the nanocrystals, **d** (and inset) the concentration (*C*) of the nanocrystals, **e** FWHM (*W*) of the fluorescence spectrum during the phosphine-free synthesis of CdSe NCs using the heating-up method. Reproduced with permission from [69]. © 2005, Wiley-VCH Verlag GmbH & Co. KGaA

evolution of the optical properties of the CdSe NCs during synthesis is shown in Fig. 6.

In the protocol of Mulvaney et al. [70], Se powder is dissolved in ODE by 2 h heating at 200 °C under inert atmosphere. After cooling to room temperature, this mixture is injected to the cadmium precursor containing solution at 300 °C. Another recent modification of the CdSe synthesis was proposed by Sapra et al. who used olive oil as the reaction medium in combination with CdO and elemental Se [71]. As can be seen from these ingredients, this method is most probably the ultimate simplification of the original protocol. The possibility to dissolve CdO in olive oil comes from the fact that oleic acid (OA) is one of its natural components. The authors used additional OA to synthesize larger-sized NCs and the obtained size range was 2.3–6.0 nm. CdTe NCs with a size of 2.5–7.0 nm have been synthesized in dodecylamine (DDA) using the classical approach based on CdMe₂ and TOP-Te [77], before protocols using non-coordinating solvents came up [69, 78, 79].

The synthesis of II-sulfide NCs (CdS, ZnS) differs somehow from those of the selenides and tellurides in terms of the applied chalcogenide sources. Elemental yellow sulfur occurs in discrete S₈ molecules, while its heavier homologues form Se_x and Te_x rings and chains, which are more difficult to solubilize. Therefore, in most syntheses, elemental sulfur, dissolved for example in ODE or oleylamine, is used as the S precursor. An illustrative example is the synthesis of a series of transition metal sulfide NCs comprising CdS and ZnS described by Joo et al. (cf. Fig. 7) [76]. At the same time, a number of appropriate monomolecular precursors, containing both the metal and the S source, are commercially available or easy to prepare. In particular

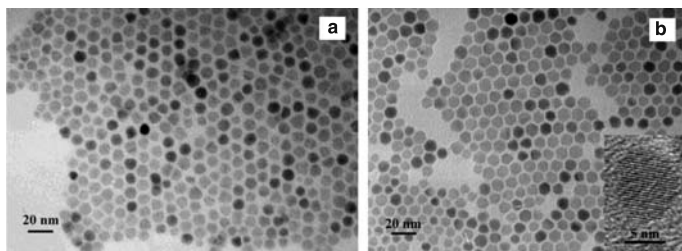


Fig. 7. TEM images of ZnS NCs synthesized via the heating-up method: **a** before size-selection process; **b** after size-selective precipitation. Inset: HRTEM image of a single ZnS NC. Reprinted with permission from [76]. © 2003 American Chemical Society

Zn or Cd xanthates and dithiocarbamates have to be mentioned in this context: most of these compounds decompose at temperatures below 200°C and are therefore suitable precursors for the preparation of transition metal sulfide NCs. Efrima and coworkers reported the use of Zn- and Cd-alkylxanthates for the synthesis of the corresponding sulfide NCs [74, 75].

Concerning zinc selenide, a promising compound for emission in the near UV/blue range, Hines and Guyot-Sionnest first reported the synthesis of ZnSe NCs showing strong band edge fluorescence in the range from 365 to 445 nm with PL Q.Y.s of 20–50% [82]. Adapting the work on CdSe NCs by Murray et al. [8] they used an organometallic zinc precursor (diethylzinc) and selenium powder dissolved in TOP (TOPSe). The major difference, with respect to the case of CdSe was the use of HDA as a solvent. TOPO turned out to bind too strongly to Zn and therefore an appropriate balance between the nucleation and the growth crucial for good size control could not be achieved. At the same time, the combination of HDA and TOP efficiently passivated the NCs' surface by removing trap states/dangling bonds, which resulted in pure band edge fluorescence.

A very simple method for the preparation of a size series of monodisperse ZnSe NCs was reported in 2004 by our group [83]. Here, pyrophoric diethylzinc was replaced by an air-stable and easy to manipulate precursor (zinc stearate), while keeping the established Se precursor (TOPSe) and using the saturated non-coordinating solvent octadecane. In the growth process zinc stearate served not only as the cation precursor but also as a source of stabilizing stearate ligands. The size of the obtained ZnSe could be varied from 3 to 7 nm by adjusting the concentration of the zinc precursor in the reaction mixture and/or varying the temperature, yielding samples emitting in the range of 390–440 nm (FWHM 12–17 nm).

Li et al. reported a similar route implying the use of a mixture of 1-octadecene and tetracosane combined with the addition of a small amount of octadecylamine (ODA) to the reaction mixture [80]. According to these authors, ODA was necessary to activate the zinc carboxylate precursor, otherwise no NCs with low size distributions could be obtained. Finally, Chen et al. used a shorter chain zinc carboxylate, namely zinc laurate generated in situ from ZnO and lauric acid in HDA. Size control of the obtained ZnSe NCs was achieved in a range of 2.5–6 nm by varying the reaction time [92]. ZnTe has been synthesized by injection of a solution containing ZnEt₂ and elemental Te in TOP into a mixture of ODA and ODE at 270°C [84]. Concerning the

mercury chalcogenides, HgTe is the only example to be prepared in organic solvents to date via the reaction of HgBr₂ and TOP-Te in a mixture of TOPO and ODA [85].

3.1.2 Ternary systems (“alloys”). As aforementioned, by taking advantage of the quantum confinement effect it is possible to tune, through size control, the fluorescence wavelength of semiconductor NCs. The formation of a ternary structure is an alternative way to influence the band gap of the NCs, not by changing their *size* but their *composition*. Although the term “alloy” is, in its strict sense, limited to solid solutions of two or more metals, it is also widely applied in literature for the description of ternary systems comprising chalcogenide ions. A typical example is Cd_{1-x}Zn_xSe, corresponding to ZnSe NCs, in which a fraction of the Zn atoms is substituted by Cd ones in the crystal lattice. The band gap of the resulting ternary alloy is in between those of pure ZnSe and of pure CdSe NCs of the same size. In contrast to the crystal lattice parameters, which show, according to Végard’s law, a linear evolution with composition, the curve describing the corresponding evolution of the band gap shows a deviation from linear behavior. However, this difference is not very pronounced for common anion systems such as Cd_{1-x}Zn_xSe or Cd_{1-x}Zn_xS [88, 89]. A measure of this deviation is the so-called bowing parameter, which depends on the difference in electronegativity of the two end components, here CdSe and ZnSe [93, 94]. Consequently, common cation alloys (CdS_{1-x}Se_x, CdSe_{1-x}Te_x) generally present larger bowing parameters than common anion ones. Different methods of the Cd_{1-x}Zn_xSe NCs synthesis were developed, deriving directly from those used for the binary compounds. While the Se precursor was generally TOPSe, the use of different Cd and Zn precursors has been explored. Organometallic approaches based on dimethylcadmium and diethylzinc were first applied [86, 87] before the recent development of a method in which only air-stable precursors (cadmium stearate and zinc stearate) were used [88]. In the case of CdSe_{1-x}S_x NCs, the influence of the nature of the solvent on the sample properties was recently studied by Al-Salim et al. [95]. The narrowing of the band gap of CdSe NCs by forming a solid solution with CdTe, further enhanced by the bowing effect, made the near IR emission range accessible [90].

3.1.3 Doped nanocrystals. Doping – the introduction of a small amount of “impurities” into the crystal lattice – is an attractive way to change the NCs’ physical properties. An important example is the doping of II–VI semiconductors with paramagnetic Mn²⁺ ions ($S = 5/2$), yielding materials denominated *dilute magnetic semiconductors* (DMS), which exhibit interesting magnetic and magneto-optical properties [96]. At the same time, the host NC can act as an antenna for the absorption of energy (e.g. light) and excitation of the dopant ions via energy transfer. In this case, mostly UV-absorbing NCs are chosen as the hosts, such as ZnS or ZnSe. Mn-doped ZnSe is an instructive example for the development of doped II–VI semiconductor NCs. Bulk ZnSe:Mn exhibits PL at 582 nm (2.13 eV), commonly assigned to an optically forbidden $d-d$ transition of Mn²⁺ (⁴T₁ to ⁶A₁) [97, 98]. This emission is

sensitive to the crystal field splitting being itself dependent on the local chemical environment.

A general problem encountered in essentially all attempts of NCs doping is the fact that the host matrix tends to expel the dopant ions to the surface, in some sort of “self-purification” process. Therefore, even in the favourable case of dopant ions, having the same valence state and similar ionic radius as the corresponding host ions, successful (volume) doping is difficult to achieve in a straightforward approach by simply adding a small amount of dopant precursor during the synthesis of the host NCs. Nevertheless, by adding dimethylmanganese [99] or manganese cyclohexanebutyrate [100] to the zinc precursor in the organometallic ZnSe synthesis [82], successful Mn-doping has been achieved, even though some residual blue emission from the ZnSe host matrix at low dopant concentrations indicated the co-existence of both doped and undoped NCs. Similarly, the injection of TBPSe into a solution of Zn- and Co-acetate in a mixture of ODE, HDA and oleic acid at 310°C led to the formation of Co^{2+} -doped ZnSe NCs [101]. However, the obtained DMS NCs contained no dopant ions in the central cores and therefore exhibited excitonic Zeeman splitting energies significantly (40%) smaller than expected from the bulk ZnSe:Co data. The same group reported recently the Co^{2+} and Mn^{2+} doping of CdSe, CdS and CdSe/CdS NCs using well-defined Cd-chalcogenide clusters [102] as starting materials [103].

A decisive step towards the understanding of the doping process was achieved by Erwin et al. who first succeeded in doping CdSe NCs with Mn^{2+} [104]. They introduced a model of doping based on kinetics and concluded that the doping mechanism is controlled by the initial adsorption of impurities on the surface of growing NCs. Only impurities remaining adsorbed on the surface for a time comparable to the reciprocal growth rate are incorporated into the NC. Three main factors influencing this residence time were determined, namely the surface morphology, NC shape and surfactants present in the growth solution. It has been shown that (0 0 1) surfaces of ZB crystals exhibit much higher impurity binding energies than the other two ZB orientations and than any facet of crystals with W or rock-salt (RS) structures. These findings were fully corroborated by the state-of-the-art, as all NCs successfully doped with Mn^{2+} ions exhibited the ZB crystal structure.

A new approach with the goal to achieve the doping of *all* NCs in a given sample was explored by Peng and coworkers. In the so-called *nucleation-doping* strategy, MnSe nuclei, formed from manganese stearate and TBPSe in octadecylamine at 280°C, were overcoated with ZnSe using zinc stearate or zinc undecylenate. No residual ZnSe emission was observed and the doped NCs exhibited thermally stable (up to 300°C) highly efficient (Q.Y. 40–70%) PL in a spectral window of 545–610 nm, depending on the ZnSe shell thickness and on the nature of the surface ligands (charged or neutral) [105]. The same approach was extended to the doping of ZnSe with Cu ions (Fig. 8) [106]. In conclusion, with exception of the comparably broad PL peaks (>50 nm at FWHM), their otherwise very interesting optical properties make transition metal-doped ZnSe NCs promising “green” alternatives to the widely studied II–VI semiconductor NCs for a number of applications including biological labeling [107].

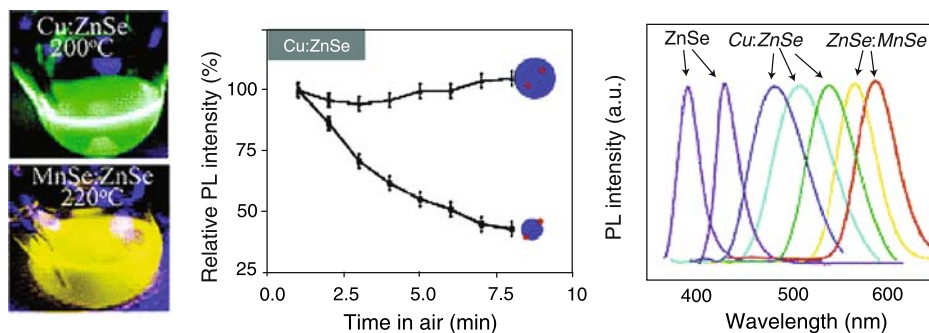


Fig. 8. Photoluminescence of Cu- and Mn-doped ZnSe NCs at high temperature (left); stability of Cu-doped ZnSe NCs in air (middle); PL spectra of ZnSe-based doped NCs. Reprinted with permission from [105]. © 2005 American Chemical Society

3.2 III–V semiconductor nanocrystals. Compared to most of the II–VI and IV–VI NCs, III–V compounds are generally referred to as “greener” NCs because the group III elements such as In or Ga are more environmentally friendly than Cd, Pb or Hg. Nevertheless, the studies and applications of III–V NCs are rather sparse as compared to their II–VI analogues, principally caused by significant difficulties in their synthesis. In fact, due to the stronger covalent bonding of the precursors generally a higher reaction temperature and a longer reaction time are necessary. These conditions favourize Ostwald ripening, leading to an increased size dispersion. Therefore, highly reactive organometallic precursors or monomolecular precursors, containing both the cation and anion already chemically bound in the same molecule, are applied in a large number of protocols.

The following section focuses on recent developments in the synthesis of mono-disperse III–V semiconductor NCs. For a more detailed description of the methods published prior to 2002 the interested reader is referred to the reviews of Green [108] and Wells and Gladfelter [109]. An overview of the different synthetic procedures is given by means of Table 3.

Table 3. Precursors, stabilizers and solvents used in the synthesis of various III–V semiconductor NCs

Material	Precursors and stabilizers	Solvent(s)	References
InP	InCl ₃ or InCl ₃ /Na ₂ C ₂ O ₄ , P(TMS) ₃	TOPO or TOPO/TOP	[110, 111]
InP, InAs	In(ac) ₃ , P(TMS) ₃ or As(TMS) ₃ , MA	ODE	[112]
InP	InMe ₃ , P(TMS) ₃ , MA	MM or DBS,	[113]
InAs	InCl ₃ , As(TMS) ₃	TOP	[114]
GaP	[Cl ₂ GaP(SiMe ₃) ₂] ₂	TOPO/TOP	[115]
GaP	Ga(<i>Pr</i> Bu ₂) ₃	TOA, HDA	[116]
GaP	GaCl ₃ , P(TMS) ₃	TOPO	[117]
GaN, AlN, InN	[M(H ₂ NCONH ₂) ₆] ₂ Cl ₃ (M=Ga, Al, In)	TOA	[118]

TMS trimethylsilyl; *ac* acetate; *MA* myristic acid; *OA* oleic acid; *TOPO* trioctylphosphine oxide; *TOP* trioctylphosphine; *ODE* 1-octadecene; *MM* methyl myristate; *DBS* dibutyl sebacate; *TOA* trioctylamine; *HDA* hexadecylamine

Most of the reports concern the synthesis of indium phosphide NCs. These are potentially an attractive alternative to CdSe or CdTe ones, due to their size-dependent emission in the visible and near infrared spectral range combined with the lower toxicity of indium with respect to cadmium. In initial synthetic routes [110, 111], the method established for cadmium chalcogenide NCs [8] was adapted to InP, but longer reaction times (3–7 days) were necessary to yield particles of good crystallinity. Interestingly, these approaches follow the heating-up method. Peng and coworkers later reported a new protocol, which is based on fatty acids as stabilizers in combination with the non-coordinating solvent ODE instead of TOPO/TOP [112]. The use of this medium provided a fast and controllable reaction, yielding high quality InP NCs. Similar results were obtained when organometallic In precursors were used in combination with ester type solvents [113]. However, to date the as-prepared NCs exhibit in all cases size dispersions exceeding 10% and the use of the expensive and pyrophoric phosphorus precursor $P(\text{TMS})_3$ (tris(trimethylsilyl)phosphine) is mandatory. NCs of the narrow band gap semiconductor InAs can be synthesized using similar approaches as in the case of InP. Both the synthesis in coordinating (TOP) [114] and non-coordinating (ODE) [112] solvent have been reported.

The synthesis of GaP NCs was reported by Mićić et al. who decomposed in a TOPO/TOP mixture a monomolecular precursor complex, $[\text{Cl}_2\text{GaP}(\text{SiMe}_3)_2]_2$, in situ generated from GaCl_3 and $P(\text{TMS})_3$ in toluene [115]. Monodispersed 8 nm GaP NCs have been synthesized from the monomolecular precursor $\text{Ga}(\text{PrBu}_2)_3$ in a mixture of trioctylamine (TOA) and HDA [116]. Depending on the concentration of HDA in the reaction medium, a shape transition from spherical to rod-like NCs has been observed. Green and O'Brien used the same monomolecular precursor in 4-ethylpyridine [119]. Furis et al. adapted the II–VI NCs hot-injection method, using GaCl_3 , $P(\text{TMS})_3$ as the gallium and phosphorus source, respectively, and TOPO as the solvent [117].

III-nitride NCs are extremely difficult to synthesize due to the absence of appropriate (i.e. highly reactive) nitrogen precursors. Further restrictions are the high growth temperature in the case of AlN and the low decomposition temperature of InN. Recent advances in this field have been achieved by Rao and coworkers [118]. They prepared AlN, InN and in particular GaN NCs of low size dispersion by the thermal decomposition of the metal–urea complexes in refluxing TOA under N_2 atmosphere.

3.3 IV–VI semiconductor nanocrystals. The IV–VI semiconductor family comprises materials of high interest for applications relying on emission in the near infrared spectral range. While only very sparse information exists concerning tin chalcogenides, their lead homologues have been intensively studied in the last years. The latter are narrow band gap semiconductors as can be seen from Table 1 (Sect. 2.4.2) and exhibit some other unique properties as compared to II–VI or III–V compounds. In particular, they show high dielectric constants, large Bohr exciton radii and the electron and hole masses are approximately equal. Two recent reviews deal with the synthesis and properties of infrared-emitting NCs, and in particular with lead chalcogenides [120, 121]. While initially significant efforts were

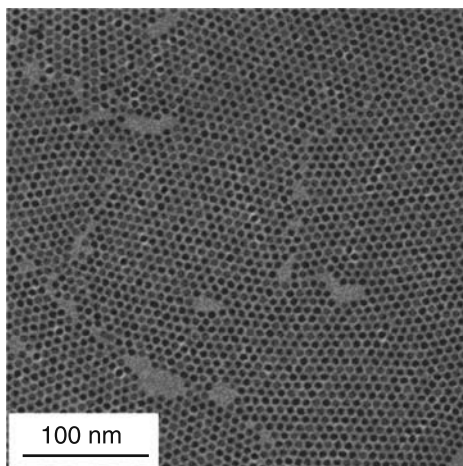


Fig. 9. TEM image of as-prepared PbSe NCs synthesized in the non-coordinating solvent ODE. The mean size is 6.8 nm and the size distribution is 6.2%. Reprinted with permission from [124]. © 2004, American Chemical Society

made to synthesize them in aqueous media, today it seems clear that the high temperature methods in organic solvents yields superior results in terms of monodispersity of the prepared NCs. In all cases the hot-injection method has been applied, and the first example was the synthesis of PbSe by Murray et al. [122]. Already successfully used in the synthesis of metal nanoparticles (e.g. Co [122], FePt [123]), a high boiling point ether (diphenylether) was applied as the solvent in combination with lead oleate (prepared in situ from lead acetate and oleic acid), while maintaining the traditional Se precursor TOPSe. The size of the NCs could be tuned within a large range (3.5–15 nm) and the monodisperse fractions obtained after size-selective precipitation exhibited size-dependent absorption spectra. The latter comprised in addition to the excitonic peak, located at 1200–2200 nm depending on the NC size, several well-defined features at higher energies. Similar as in the case of II–VI compounds, the synthetic scheme was later modified by using the non-coordinating solvent ODE [124]. Figure 9 shows a TEM image of the PbSe NCs obtained with this method. They exhibit a narrow size dispersion (5–7%) without the necessity of fractionation procedures such as size-selective precipitation.

In 2003, the synthesis of PbS NCs by the hot-injection method was first published by Hines and Scholes [125]. In this case the non-coordinating solvent ODE was applied in combination with OA as the stabilizer and PbO and $(\text{TMS})_2\text{S}$ as the Pb and S precursors, respectively. The pronounced excitonic peak visible in the presented absorption spectra spans a wavelength range from 800 to 1800 nm as a function of the NC size and narrow emission linewidths have been reported. In the meantime, a number of derived synthetic protocols have been published. Table 4 gives an overview of the explored experimental parameters. Concerning PbTe, essentially the same procedures as those developed for PbSe have been successfully adapted to yield NCs with narrow size distributions of 5–7% [126, 127]. Depending on the reaction parameters, instead of spherical particles a variety of different shapes can be

Table 4. Precursors, stabilizers and solvents used in the synthesis of various IV–VI semiconductor NCs

Material	Precursors and stabilizers	Solvent	References
PbSe	Pb(ac) ₂ , OA, TOP-Se	DPE	[122, 128–132]
PbSe	Pb(chbt) ₂ , TBP-Se	TOPO	[133]
PbSe	PbO, OA, TOP-Se	ODE	[124]
PbS	PbO, OA, (TMS) ₂ S	ODE	[125]
PbS	PbCl ₂ , S/OAm	OAm	[76]
PbTe	Pb(ac) ₂ , OA, TOP-Te	DPE	[126]
PbTe	PbO, OA, TOP-Te	ODE	[127]

TMS trimethylsilyl; *ac* acetate; *chbt* cyclohexylbutyrate; *OA* oleic acid; *OAm* Oleylamine; *DPE* diphenylether

obtained, such as cubes or stars. In this context, the paper of Houtepen et al. has to be cited, which revealed the crucial role of the concentration of acetate in the reaction medium on the NC shape [128].

3.4 Nanocrystals of other semiconductors. Apart from III–V QDs, ternary semiconductor NCs such as I–III–VI₂ type chalcopyrites (CuInSe₂-CISE, CuInS₂-CIS) represent further potential alternative materials to cadmium-based systems. They are direct semiconductors and exhibit a relatively low band gap (1.05 eV for CISE, 1.5 eV for CIS). CIS and CISE NCs were intensively studied because of their high potential for use in photovoltaics [134–136]. To the contrast, their PL properties were rarely investigated in previous reports [137, 138]. Recently Castro et al. reported a new synthesis method for CIS via the decomposition of the single source precursor (PPh₃)₂CuIn(SEt)₄, yielding luminescent CIS samples with a PL Q.Y. of ca. 5% [139, 140]. The Hyeon group prepared large-sized CIS NCs of anisotropic shape from Cu- and In-oleate in a mixture of oleylamine and dodecanethiol via the heating-up method [141]. Nakamura et al. doped CIS NCs with Zn and were able to vary their PL wavelength from 570 to 800 nm, with Q.Y.s in the range of 5% [142]. Increased fluorescence Q.Y. upon addition of Zn has also recently been observed in another example of a I–III–VI₂ semiconductor: a solid solution of ZnS and AgInS₂ exhibited strong, tunable emission in the visible range [143]. An early approach for the synthesis of CISE comprised the use of copper(I) and indium chloride in TOPO, and the injection of TOP-Se [144]. More recently, CISE NCs have been prepared in the non-coordinating solvent ODE [145].

The synthesis of the elemental semiconductors Si and Ge is by far less-developed than that of the other semiconductor families discussed. This fact stands out against their technological importance. An inspection of the relevant literature seems to indicate that the synthesis in supercritical solvents [18, 146–149] or the use of the microemulsion technique [150, 151] are more appropriate than the preparation of these materials in organic solvents using the hot-injection or the heating-up method. An exception from this rule is the approach of Kauzlarich and coworkers, who used the metathesis reaction of the Zintl salts NaGe and KGe or of Mg₂Ge with excess GeCl₄ in refluxing glyme (ethylene glycol dimethyl ether), diglyme or triglyme for the preparation of Ge NCs [152]. The same group applied a similar procedure

comprising Mg_2Si , SiCl_4 and glyme for the synthesis of Si NCs [153]. In an earlier report, Heath et al. prepared Ge NCs via the reduction of chlorogermanes and organochlorogermanes by a K/Na alloy in heptane, followed by thermal annealing in an autoclave at 270°C [154].

4. Core/shell systems

The following section is dedicated to the description of the synthesis of CS NCs. Core multiple shell structures such as core/shell/shell NCs or quantum-dot-quantum-well onion-like systems are considered in a separate Chapter of Dorfs and Eychmüller.

4.1 Type I systems. As already mentioned in Sect. 2, type I systems are generally synthesized with the goal to increase the fluorescence Q.Y. and stability against photo-bleaching by improving NCs' surface passivation. Unlike otherwise stated, the shell precursors are slowly injected to a dispersion of the purified core NCs.

4.1.1 Synthesis of core/shell nanocrystals of II–VI semiconductors. One of the earliest CS structures reported was CdSe/ZnS, which is at the same time the most intensively studied system to date. Its synthesis was first described by Hines and Guyot-Sionnest who overcoated 3 nm CdSe NCs with 1–2 monolayers of ZnS, resulting in a Q.Y. of 50% [40]. ZnS shell growth has been achieved by the injection of a mixture of the organometallic precursors diethylzinc and hexamethyldisilathiane, also known as bis(trimethylsilyl)sulfide, $\text{S}(\text{TMS}_2)$ at high temperature (300°C). A whole size series of CdSe/ZnS NCs and their in depth characterization was published shortly afterwards by Bawendi's group [41]. A similar approach has later been applied for the ZnS capping of CdSe nanorods with lengths up to 30 nm [155]. The addition of HDA to the traditionally used solvent system TOPO/TOP led to a better control of the growth kinetics during both the CdSe core and ZnS shell synthesis resulting in a lower size distribution and Q.Y.s of the order of 60% (cf. Fig. 10) [33]. Very recently extremely small CdSe/ZnS CS NCs have been synthesized by Kudera et al., making the blue spectral region accessible with this system [156]. The synthetic approach was based on the sequential growth of CdSe magic size clusters in a mixture of trioctylphosphine, dodecylamine, and nonanoic acid at temperatures of 80°C and their subsequent overcoating with ZnS. Another procedure to access this spectral region was suggested by Jun and Jang [157]: by carrying out the ZnS overgrowth process at 300°C using precursors (zinc acetate and octanethiol) of relatively low reactivity, shell material diffused into the core resulting in a significant hypsochromic shift of the emission wavelength. The obtained NCs emit at 470 nm with a Q.Y. of 60%. Multimodal CS NCs appropriate for both optical and magnetic resonance imaging techniques have been obtained by doping of the ZnS shell with manganese ions in the range of 0.6–6.2% [158]. In this case, the growth of the $\text{Zn}_{1-x}\text{Mn}_x\text{S}$ shells of 1–6 monolayer thickness was achieved by injection of a mixture of diethylzinc, dimethylmanganese and H_2S gas to a dispersion of the CdSe core NCs at 170°C .

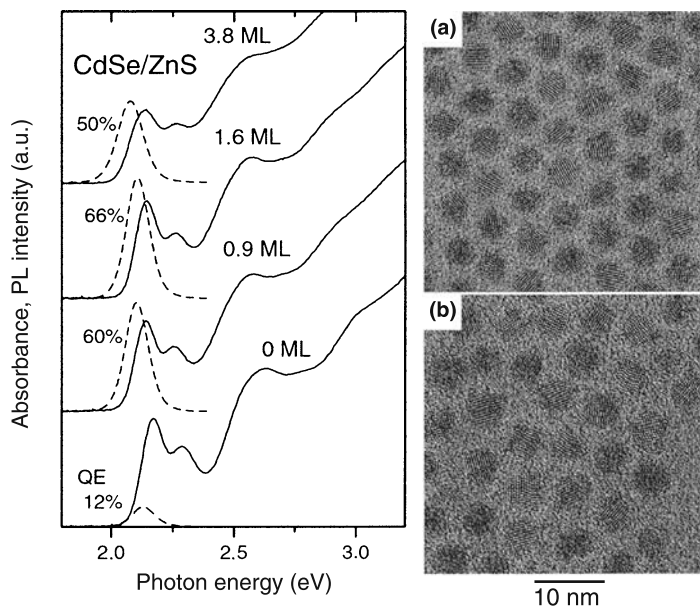


Fig. 10. Left panel: UV-vis absorption and PL spectra during the growth of a ZnS shell (ML = monolayer) on 4 nm CdSe NCs. Right panel: TEM images of 4 nm core NCs (a) and of CdSe/ZnS CS NCs (b; 1.6 ZnS ML). Reprinted with permission from [33]. © 2001, American Chemical Society

A further CdSe-based system exhibiting a different band alignment is CdSe/CdS. In this common cation heterostructure, a large band offset for the holes is combined with a relatively small one for the electrons. Epitaxial growth is favoured by the comparably small lattice mismatch of around 4% between the core and shell material. Peng et al. reported the synthesis and detailed characterization of series of CdSe/CdS NCs with core diameters ranging from 2.3 to 3.9 nm and Q.Y.s above 50% [42]. In contrast to the CdSe/ZnS system, exhibiting a rather small bathochromic shift (5–10 nm) of the excitonic and PL peak upon shell growth, here these features are continuously shifting throughout the shell growth, indicating a delocalization of the electron over the entire CS structure. While in this early report organometallic precursors (dimethylcadmium, bis(trimethylsilyl)sulfide) had been used, more recently the synthesis of this CS system was carried out using air-stable precursors, i.e. cadmium oleate and elemental sulfur dissolved in ODE [66]. O'Brien and coworkers extended their work on monomolecular precursors to the CdSe/CdS CS system using bis(hexyl(methyl)dithiocarbamate) and bis(hexyl(methyl)disele-nocarbamate) cadmium compounds for the core NC and shell growth, respectively [159, 160]. Another modification of the original protocol [40] concerned the omission of the intermediate purification step of the core NCs and growth of the CS structure in a so-called one-pot synthesis, yielding NCs with Q.Y.s in the range of 50–85% [161]. In addition, alternative precursors for the shell growth have been proposed in the same article, namely in situ generated H_2S gas and cadmium acetate. The preparation of particularly small CdSe/CdS CS NCs with core sizes in the range of 1.2–1.5 nm, emitting in the range of 445–517 nm with Q.Y.s of 60–80%, has been

described by Pan et al. [162]. Both core and shell synthesis were carried out at 180/140°C in an autoclave using cadmium myristate and selenourea/thiourea as precursors, oleic acid as a stabilizer and a toluene/water two phase solvent.

CdSe/ZnSe is a CS system exhibiting, in contrast to CdSe/CdS, efficient confinement of the electrons in the NC core due to the large conduction band offset, while only a relatively small barrier exists for the holes. Although the lattice mismatch is slightly larger than in CdSe/CdS (6.3 vs. 3.9%), the common anion structure is particularly favourable for epitaxial-type shell growth. While in earlier work on CdSe/ZnSe NCs rather low values of the PL Q.Y. (<1%) were published [163], our group reported more recently a modified synthesis method using for the first time the air-stable precursor zinc stearate instead of diethylzinc as the zinc source in combination with selenium dissolved in trioctylphosphine (TOPSe) as the Se source [164]. The obtained CS NCs exhibited Q.Y.s in ranging from 60 to 85% and narrow emission linewidths. Lee et al. studied the effect of lattice distortion in the CdSe/ZnSe CS system on the optical spectra by varying the concentration of the ZnSe precursor solution used for the shell growth [165] as well as the ripening kinetics upon thermal annealing [166].

Both CdSe/CdS and CdSe/ZnSe heterostructures exhibit high fluorescence Q.Y.s and can have specific interests due to the “accessibility” of the weakly confined electrons or holes, respectively. On the other hand, if purely high stability of the optical properties against photo-degradation and chemical inertness of the shell material are desired, zinc sulfide is the shell material of choice. Although it is in principle possible to obtain green or even blue emission with CdSe NCs of small size, their capping with ZnS has only very recently been achieved [156]. As a matter of fact, an analysis of the present state of the art suggests that for a large variety of materials the preparation of CS NCs of low size dispersion and satisfying optical properties is facilitated when core NCs with diameters in the range of approximately 2.5 and 5 nm are used. Consequently the synthesis of other types of core NCs than CdSe has been developed with the goal to better cover the green/blue/UV (and the near infrared) spectral region. In this context, an attractive alternative to the tuning of the emission colour with size is the formation of alloy structures, allowing for the colour variation by changing the composition of the NCs. An example are $\text{Cd}_{1-x}\text{Zn}_x\text{Se}$ NCs, whose band gap can be varied by changing x between the values of pure CdSe and pure ZnSe NCs of the same size. This system is particularly interesting for the fabrication of efficient green emitters for use in display applications. To do so, the alloy core NCs have been overgrown with a ZnS shell either using the established diethylzinc/bis(trimethylsilyl)sulfide method [87] or, more recently, by means of the air-stable monomolecular precursor zinc diethylxanthate [88]. In the latter case, after the growth of three ZnS monolayers, the obtained CS NCs emitted at 530 nm with a linewidth of 35 nm (FWHM) and a Q.Y. of 65%.

Emission wavelengths in the blue and near UV spectral region have been obtained by using larger band gap core materials, in particular CdS and ZnSe. CdS NCs have been overgrown with a ZnS shell using the classical organometallic approach with dimethylcadmium and $\text{S}(\text{TMS})_2$ as precursors, yielding an emission in the range of 460–480 nm (FWHM 24–28 nm) with Q.Y.s in of 20–30% [167]. Recently these reagents were replaced by a combination of the air-stable monomolecular precursor

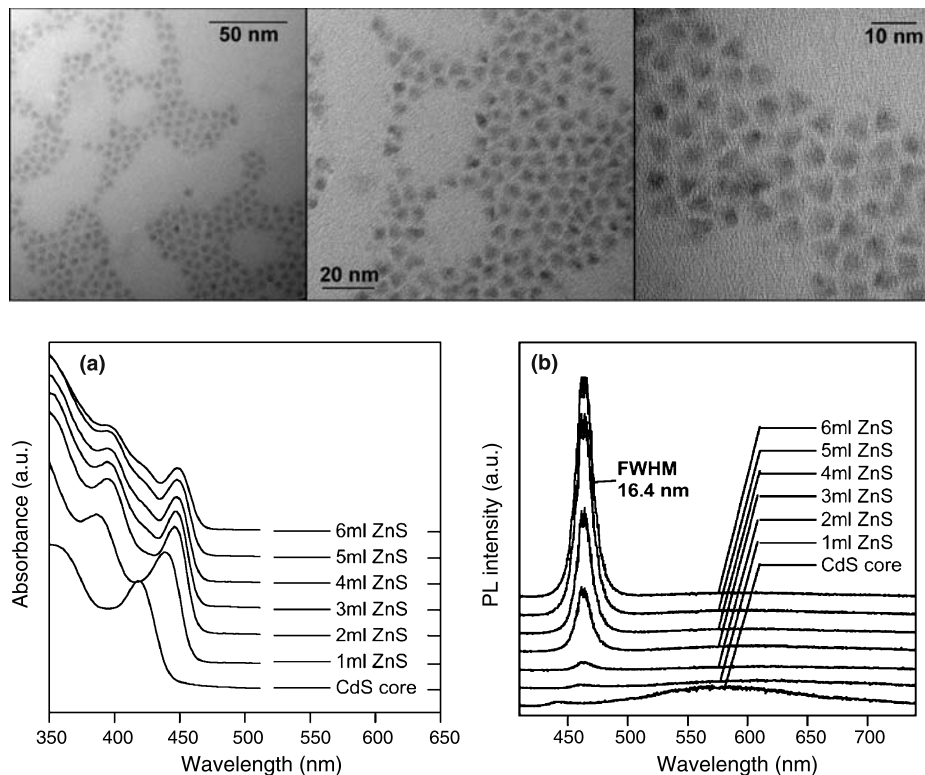


Fig. 11. Top: TEM images at different magnifications of CdS/ZnS NCs using zinc ethylxanthate as precursor for the ZnS shell growth. Bottom: **a** UV-vis absorption spectra; **b** PL spectra recorded during the addition of 6 mL of the ZnS precursor solution corresponding to the growth of a five monolayer-thick ZnS shell on 4 nm CdS core NCs [168]

zinc ethylxanthate and zinc stearate, resulting in monodisperse CdS/ZnS CS NCs emitting in the range of 440–480 nm (15–18 nm FWHM) with Q.Y.s of 35–45% (Fig. 11) [168].

The CdS core NCs have further been used as a host matrix for Mn dopant ions in CdS:Mn/ZnS CS systems [169]. ZnSe has equally been overcoated by ZnS using organometallic precursors, leading to emission wavelengths in the range of 400 nm, PL linewidths of 20 nm and Q.Y.s of the order of 15% [170]. In a newer approach based on the use of alternative precursors, i.e. ZnO and TOPSe for the core NCs and zinc laurate and TOPS for the shell growth carried out at 180°C in HDA, Q.Y.s up to 30% were reached [171].

Cadmium telluride, exhibiting a smaller bulk band gap than cadmium selenide (1.5 vs. 1.75 eV at 300 K), is in principle a good candidate for the fabrication of red or near infrared-emitting quantum dots. However, due to the high oxidation sensitivity of CdTe NCs prepared in organic solvents, comparably few reports exist concerning the preparation of related CS systems in organic solvents, such as CdTe/ZnS [172]. In this work, CdTe core NCs were synthesized in water following the recipe of [14] and

transferred to organic solvent by ligand exchange before overgrowing them with the ZnS shell.

4.1.2 Synthesis of core/shell nanocrystals of III–V semiconductors. Literature on III–V semiconductor based CS systems is much more sparse than in the case of II–VI compounds, as a consequence of the lack of robust synthesis methods for most core NCs of this family (cf. Sect. 3.2). As-prepared InP NCs exhibit rather poor optical properties as compared to CdSe. The PL linewidth is significantly broader, of the order of 50 nm (FWHM), and in addition to band edge emission peaks related to defect state emission occur in the spectrum. Furthermore, the Q.Y. is low, typically inferior to 1%. Talapin et al. described an efficient way to increase the Q.Y. of InPNCs to values approaching 40% by photo-assisted etching of their surface with HF [37]. This process resulted in the removal of surface phosphorous atoms being at the origin of trap states, which provided non-radiative recombination pathways. Concerning InP-based CS systems, Haubold et al. used organometallic precursors to grow a ZnS shell on InP and observed a subsequent increase of the Q.Y. in a slow room temperature process to 15% after 3 days and to 23% after 3 weeks [173]. In order to adjust the lattice parameters of the core and shell materials and to reduce strain-induced defects, Mičić et al. developed a CdZnSe₂ shell leading to a fluorescence Q.Y. of 5–10% [174]. Cao and Banin reported the preparation of several CS systems based on near infrared-emitting InAs core NCs, including InP, GaAs, CdSe, ZnSe and ZnS using high-temperature pyrolysis of organometallic precursors in TOPO [175, 176]. The obtained fluorescence Q.Y.s depended on the shell material. In the case of InP, PL quenching was observed, whereas ZnS led to 8% and for CdSe and ZnSe an enhancement up to 20% was detected. More recently the synthesis of a series of small InAs/ZnSe CS NCs has been described, aiming at emission wavelengths in the range of 700–900 nm [177]. This spectral region is especially well-adapted for in vivo biological imaging due to the reduced light scattering by the tissue. The obtained NCs exhibited a Q.Y. of 6–9% after transfer to the aqueous phase and were successfully applied for the in vivo imaging of lymph nodes.

4.1.3 Synthesis of core/shell nanocrystals of IV–VI semiconductors. In contrast to the discussed II–VI and III–V semiconductors exhibiting either the hexagonal wurtzite or the cubic zinc blende crystal structure, the IV–VI family is characterized by the rocksalt structure (cf. Table 1). Only lead-based NCs (PbS, PbSe) have been studied in form of CS systems. Lifshitz and coworkers reported the synthesis of PbSe/PbS and PbSe/PbSe_xS_{1-x} CS NCs emitting in the range of 1–2 μm with Q.Y.s of 40–50% and 65%, respectively, by means of the use of lead(II)acetate, TOPSe and TOPS as precursors, oleic acid as stabilizer and diphenylether as the solvent (Fig. 12) [178–180]. The SILAR method mentioned before in the case of CdSe/CdS has recently been applied for the synthesis of PbSe/PbS NCs [181].

4.2 Type II systems. Research on colloidal type II systems was triggered by the seminal work of Bawendi et al. [182] who described the synthesis and optical properties of CdTe/CdSe and CdSe/ZnTe CS NCs [182]. The emission wavelength of

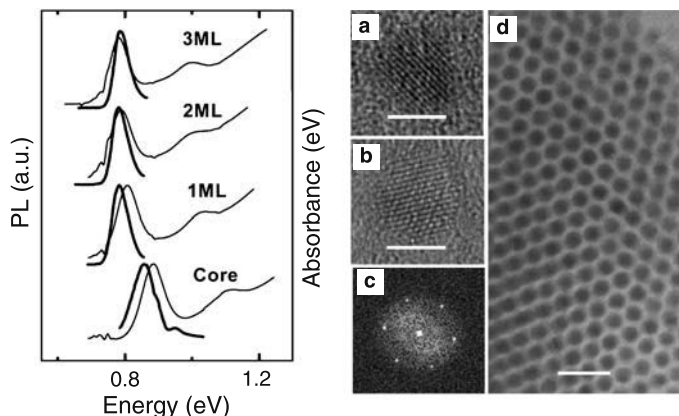


Fig. 12. Left panel: Evolution of the UV-vis absorption and PL spectra of 4.9 nm PbSe core NCs during the growth of a PbS shell of indicated thickness. Right panel: **a** HRTEM image of a PbSe/PbS CS NC comprising a 4.8 nm core and a 1.2 nm shell; **b** HRTEM image of a PbSe/PbSe_{0.5}S_{0.5} core/alloyed shell NC; **c** FFT image of the particle in image A; **d** TEM image of self-assembled 6.7 nm core/alloyed shell NCs. The scale bars are 5 nm in **a** and **b**, and 20 nm in **d**. Reprinted with permission from [180]. © 2006 American Chemical Society

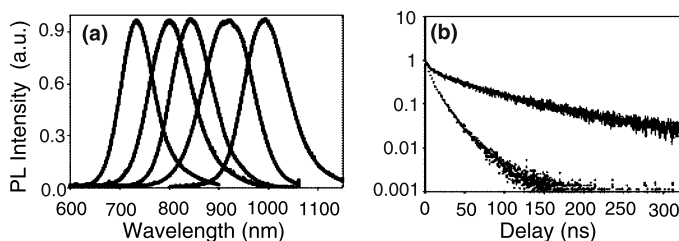


Fig. 13. **a** Normalized PL spectra of CdTe/CdSe CS NCs having the core/shell radii of 1.6/1.9, 1.6/3.2, 3.2/1.1, 3.2/2.4, and 5.6/1.9 nm (from left to right). **b** Normalized PL decays of 3.2/1.1 nm CdTe/CdSe CS NCs and of the corresponding 3.2 nm CdTe core NCs (dotted line). Reprinted with permission from [182]. © 2003 American Chemical Society

CdTe/CdSe NCs could be tuned by changing the shell thickness and the core NC size from 700 to 1000 nm (Fig. 13). This approach is an alternative possibility to shift the emission peak to higher wavelengths, which would not be attainable by simply increasing the size of the core NC in a type I CS system. On the other hand the observed mean decay lifetime (57 ns) was significantly larger than that of the corresponding core CdTe NCs (9.6 ns), and the Q.Y. was low (4 %) with respect to type I CS systems. CdTe/CdSe CS NCs were further synthesized without the use of organometallic precursors applying CdO, TOPTe and TOPSe, leading to Q.Y.s approaching 40% for small shell thicknesses below 0.5 nm [183]. Similarly, CdSe/ZnTe NCs have been prepared with CdO as the cadmium precursor and femtosecond dynamics measurements revealed that the rate of photo-induced electron/hole spatial separation decreased with increasing core size and is independent of the shell thickness [184].

Klimov and coworkers first studied the optical properties of so-called “inverted” CS NCs, i.e. the band gap of the core material (ZnSe) is larger than that of the shell

material (CdSe) [185]. On the basis of the radiative recombination lifetimes recorded for NCs with a fixed core size and increasing shell thickness, a continuous transition from type I (both electron and hole wave functions are distributed over the entire NC) to type II (electron and hole are spatially separated between the shell and the core) and back to type I (both electron and hole primarily reside in the shell) localization regimes was observed. The samples exhibited emission in the range of 430–600 nm and Q.Y.s of 60–80%. The same CS system was also synthesized applying CdO dissolved with oleic acid in octadecane and TOPSe as the shell precursors [186]. By varying the CdSe shell thickness on 2.8 core ZnSe NCs, the emission wavelength could be tuned in a broad spectral range (417–678 nm) with Q.Y.s of 40–85%. Furthermore size focusing during the shell growth has been observed in contrast to the usually occurring broadening of the size distribution at this stage of the reaction. ZnTe/CdTe represents the first common anion type II system, reported by Basché coworkers [187]. The same article also comprises the synthesis of ZnTe NCs with CdS and CdSe shells. These heterostructures were obtained by addition of precursors (cadmium oleate, TOPTe, TOPSe or sulfur dissolved in octadecane) to the crude dispersion of ZnTe core NCs. Q.Y.s of up to 30% have been observed and the emission could be tuned in the range of 500–900 nm. Interestingly, the same group observed in the case of the ZnTe/CdSe CS system, also described in [188], a transition from the concentric CS structure via pyramidal to tetrapod-shaped heterostructures when the shell growth was carried out at 215°C instead of 240°C (cf. Fig. 14) [189].

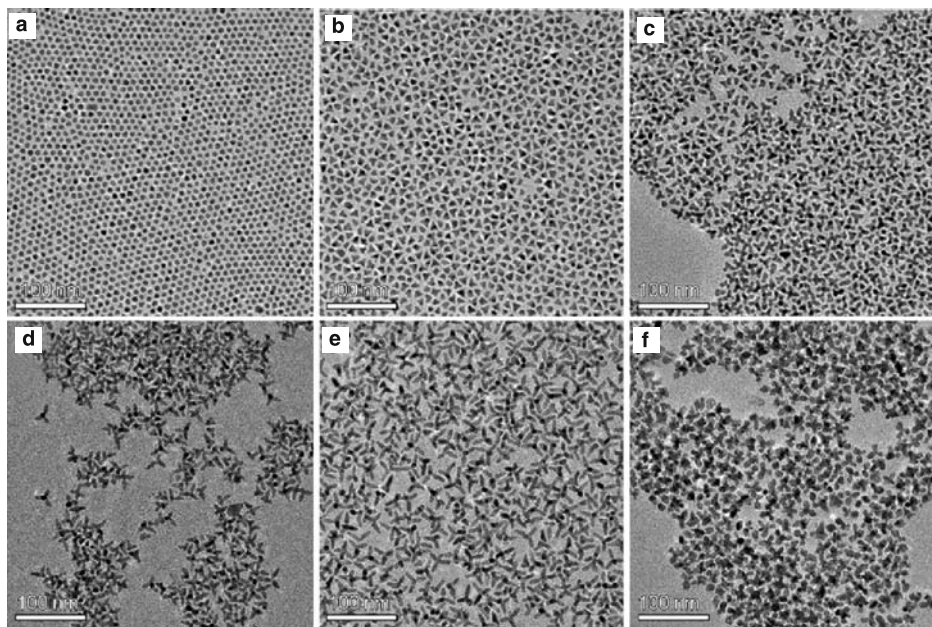


Fig. 14. TEM images of ZnTe/CdSe NCs: transition from **a** slightly anisotropic core/shell to **b** pyramidal to **c, d, e** tetrapod-shaped heterostructures with different arm lengths. **f** TEM image of tetrapod-shaped ZnTe/CdS NCs. Reproduced with permission from [189]. © 2006 Wiley–VCH Verlag GmbH & Co. KGaA

5. Conclusions and outlook

The synthesis of cadmium chalcogenide NCs via the hot-injection method reported in 1993 [8] was the starting shot for an impressive evolution of this research field. Within the last 15 years the synthesis of monodisperse spherical NCs of a large variety of semiconductors has been achieved. Moreover, the same synthetic scheme allows for the preparation of shape-controlled anisotropic NCs (e.g. rod-like or branched structures) [190, 191] and of composition-controlled ternary compounds (“alloy” semiconductors). For all materials, an ongoing trend toward the simplification of the synthesis procedure can be observed in view of an enhanced reproducibility and scale-up of the reactions. As a consequence, recent advances comprise the substitution of pyrophoric precursors by air-stable ones and the use of the heating-up technique instead of the hot-injection method. However, most of the published work to date is dedicated to the II–VI semiconductor family, and in particular to cadmium chalcogenides. The latter have an extremely low acceptability for technological applications due to the toxicity of cadmium and related problems with the handling of these compounds. To give an example, the use of toxic elements such as Cd, Pb and Hg has been severely limited by recent restrictions established in the European Union¹. Therefore it is necessary to develop robust synthesis methods for NCs of alternative semiconductor materials. Ternary semiconductors such as chalcopyrites or doped NCs (e.g. ZnSe:Mn) may gain importance in this context. Still important challenges remain for the synthetic chemist. When moving for example from the II–VI family to the more covalently bound III–V compounds, it is much more difficult to produce monodisperse samples. Furthermore, hot-injection or heating-up synthesis methods for NCs of several technologically highly important materials are completely lacking up till now, such as gallium nitride or silicon, to name a few. The successful rational design of new synthesis strategies implies a better understanding of the NCs’ formation mechanisms, which can be achieved by the precise investigation of their nucleation and growth processes.

In view of the developments in the domain of CS semiconductor NCs in the last decade, it can be speculated that a large variety of new heterostructures with exciting and, in some cases unprecedented features will be synthesized by chemical routes in the next years. The ability to precisely control the shell thickness will further boost advances in the preparation of core/shell/shell or other complex structures, such as quantum-dot-quantum-wells. Significant progress has also been achieved in the field of anisotropic shell growth on spherical CdSe NCs, leading to new rod-shaped CS nanostructures, which combine unique optical properties (high Q.Y., polarized emission) with appealing self-assembly properties [192, 193]. The reported synthetic procedure using small core NCs as seeds in the so-called seeded-growth approach, opens up the way for the generation of new heterostructures, including nanorods and branched ones, such as bi-, tri-, tetra-pods or multipods. Similar as in the case of II–VI compounds, it can be expected that a growing number of CS systems based on III–V semiconductors will be developed, inspired by the huge amount of research carried out in the field of III–V nanostructures grown by molecular beam epitaxy

¹ cf. the Reduction of Hazardous Substances (RoHS) mandate, banning the use of six chemicals – including Cd, Hg, Cr^{VI} and Pb – in almost all electronics products (date of effect: 01/07/2006).

(MBE) techniques. Finally, the association of semiconductors with other materials such as metals or oxides in the same CS heterostructure allows for the design of NCs combining different physical properties, e.g. fluorescence, magnetism, etc. In such a manner, novel functional building blocks can be generated for applications in fields ranging from (opto-)electronics via information technology to healthcare. In most of these examples, the NCs are used as a platform for further surface functionalization, enabling their integration into devices or materials, or their binding to other molecules or macromolecules.

References

- [1] Brus LE (1984) Electron–electron and electron–hole interactions in small semiconductor crystallites – the size dependence of the lowest excited electronic state. *Journal of Chemical Physics* 80: 4403–4409
- [2] Bawendi MG, Steigerwald ML, Brus LE (1990) The quantum-mechanics of larger semiconductor clusters (um dots). *Annual Review of Physical Chemistry* 41: 477–496
- [3] Efros AL, Rosen M, Kuno M, Nirmal M, Norris DJ, Bawendi M (1996) Band-edge exciton in quantum dots of semiconductors with a degenerate valence band: dark and bright exciton states. *Physical Review B* 54: 4843–4856
- [4] Efros AL, Efros AL (1982) Interband absorption of light in a semiconductor sphere. *Soviet Physics Semiconductors—USSR* 16: 772–775
- [5] Henglein A (1982) Photo-degradation and fluorescence of colloidal-cadmium sulfide in aqueous-solution. *Berichte der Bunsen-Gesellschaft-Physical Chemistry Chemical Physics* 86: 301–305
- [6] Rossetti R, Brus L (1982) Electron–hole recombination emission as a probe of surface-chemistry in aqueous cds colloids. *Journal of Physical Chemistry* 86: 4470–4472
- [7] Rossetti R, Nakahara S, Brus LE (1983) Quantum size effects in the redox potentials, resonance Raman-spectra, and electronic-spectra of CdS crystallites in aqueous-solution. *Journal of Chemical Physics* 79: 1086–1088
- [8] Murray CB, Norris DJ, Bawendi MG (1993) Synthesis and characterization of nearly monodisperse CdE (E = S, Se, Te) semiconductor nanocrystallites. *Journal of the American Chemical Society* 115: 8706–8715
- [9] Murray CB, Kagan CR, Bawendi MG (2000) Synthesis and characterization of monodisperse nanocrystals and close-packed nanocrystal assemblies. *Annual Review of Materials Science* 30: 545–610
- [10] Yin Y, Alivisatos AP (2005) Colloidal nanocrystal synthesis and the organic-inorganic interface. *Nature* 437: 664–670
- [11] Green M (2005) Organometallic based strategies for metal nanocrystal synthesis. *Chemical Communications* 24: 3002–3011
- [12] Park J, Joo J, Kwon SG, Jang Y, Hyeon T (2007) Synthesis of monodisperse spherical nanocrystals. *Angewandte Chemie-International Edition* 46: 4630–4660
- [13] Rogach AL, Talapin DV, Shevchenko EV, Kornowski A, Haase M, Weller H (2002) Organization of matter on different size scales: monodisperse nanocrystals and their superstructures. *Advanced Functional Materials* 12: 653–664
- [14] Rogach AL, Franzl T, Klar TA, Feldmann J, Gaponik N, Lesnyak V et al (2007) Aqueous synthesis of thiol-capped CdTe nanocrystals: state-of-the-art. *Journal of Physical Chemistry C* 111: 14628–14637
- [15] Pileni MP (1997) Nanosized particles made in colloidal assemblies. *Langmuir* 13: 3266–3276
- [16] Wang X, Peng Q, Li YD (2007) Interface-mediated growth of monodispersed nanostructures. *Accounts of Chemical Research* 40: 635–643
- [17] Biswas K, Rao CNR (2007) Use of ionic liquids in the synthesis of nanocrystals and nanorods of semiconducting metal chalcogenides. *Chemistry-A European Journal* 13: 6123–6129
- [18] Shah PS, Hanrath T, Johnston KP, Korgel BA (2004) Nanocrystal and nanowire synthesis and dispersibility in supercritical fluids. *Journal of Physical Chemistry B* 108: 9574–9587
- [19] Gaponenko SV (1998) *Optical properties of semiconductor nanocrystals*. Cambridge University Press, Cambridge (UK)
- [20] Norris DJ, Sacra A, Murray CB, Bawendi MG (1994) Measurement of the size-dependent hole spectrum in CdSe quantum dots. *Physical Review Letters* 72: 2612–2615

- [21] Reiss P, Bleuse J (unpublished)
- [22] Ekimov AI, Hache F, Schanne-Klein MC, Ricard D, Flytzanis C, Kudryavtsev IA et al (1993) Absorption and intensity-dependent photoluminescence measurements on CdSe quantum dots – assignment of the 1st electronic-transitions. *Journal of the Optical Society of America B-Optical Physics* 10: 100–107
- [23] Nirmal M, Norris DJ, Kuno M, Bawendi MG, Efros AL, Rosen M (1995) Observation of the dark exciton in CdSe quantum dots. *Physical Review Letters* 75: 3728–3731
- [24] Mason MD, Credo GM, Weston KD, Buratto SK (1998) Luminescence of individual porous Si chromophores. *Physical Review Letters* 80: 5405–5408
- [25] Pistol ME, Castrillo P, Hessman D, Prieto JA, Samuelson L (1999) Random telegraph noise in photoluminescence from individual self-assembled quantum dots. *Physical Review B* 59: 10725–10729
- [26] VandenBout DA, Yip WT, Hu DH, Fu DK, Swager TM, Barbara PF (1997) Discrete intensity jumps and intramolecular electronic energy transfer in the spectroscopy of single conjugated polymer molecules. *Science* 277: 1074–1077
- [27] Xie XS, Trautman JK (1998) Optical studies of single molecules at room temperature. *Annual Review of Physical Chemistry* 49: 441–480
- [28] Dickson RM, Cubitt AB, Tsien RY, Moerner WE (1997) On/off blinking and switching behaviour of single molecules of green fluorescent protein. *Nature* 388: 355–358
- [29] Kuno M, Fromm DP, Hamann HF, Gallagher A, Nesbitt DJ (2000) Nonexponential “blinking” kinetics of single CdSe quantum dots: a universal power law behavior. *Journal of Chemical Physics* 112: 3117–3120
- [30] Chepic DI, Efros AL, Ekimov AI, Vanov MG, Kharchenko VA, Kudryavtsev IA et al (1990) Auger ionization of semiconductor quantum drops in a glass matrix. *Journal of Luminescence* 47: 113–127
- [31] Empedocles S, Bawendi M (1999) Spectroscopy of single CdSe Nanocrystallites. *Accounts of Chemical Research* 32: 389–396
- [32] Neuhauser RG, Shimizu KT, Woo WK, Empedocles SA, Bawendi MG (2000) Correlation between fluorescence intermittency and spectral diffusion in single semiconductor quantum dots. *Physical Review Letters* 85: 3301–3304
- [33] Talapin DV, Rogach AL, Kornowski A, Haase M, Weller H (2001) Highly luminescent monodisperse CdSe and CdSe/ZnS nanocrystals synthesized in a hexadecylamine–trioctylphosphine oxide–trioctylphosphine mixture. *Nano Letters* 1(4): 207–211
- [34] Munro AM, Plante IJL, Ng MS, Ginger DS (2007) Quantitative study of the effects of surface ligand concentration on CdSe nanocrystal photoluminescence. *Journal of Physical Chemistry C* 111: 6220–6227
- [35] Jang E, Jun S, Chung YS, Pu LS (2004) Surface treatment to enhance the quantum efficiency of semiconductor nanocrystals. *Journal of Physical Chemistry B* 108: 4597–4600
- [36] Micić OI, Cheong HM, Fu H, Zunger A, Sprague JR, Mascarenhas A, Nozik AJ (1997) Size-dependent spectroscopy of InP quantum dots. *Journal of Physical Chemistry B* 101(25): 4904–4912
- [37] Talapin DV, Gaponik N, Borchert H, Rogach AL, Haase M, Weller H (2002) Etching of colloidal InP nanocrystals with fluorides: photochemical nature of the process resulting in high photoluminescence efficiency. *Journal of Physical Chemistry B* 106(49): 12659–12663
- [38] Yeh CY, Lu ZW, Froyen S, Zunger A (1992) Zinc-blende-wurtzite polytypism in semiconductors. *Physical Review B* 46: 10086–10097
- [39] Jacobs K, Wickham J, Alivisatos AP (2002) Threshold size for ambient metastability of rocksalt CdSe nanocrystals. *Journal of Physical Chemistry B* 106: 3759–3762
- [40] Hines MA, Guyot-Sionnest P (1996) Synthesis and characterization of strongly luminescing ZnS-capped CdSe nanocrystals. *Journal of Physical Chemistry* 100: 468–471
- [41] Dabbousi BO, Rodriguez Viejó J, Mikulec FV, Heine JR, Mattoussi H, Ober R et al (1997) (CdSe) ZnS core-shell quantum dots: synthesis and characterization of a size series of highly luminescent nanocrystallites. *Journal of Physical Chemistry B* 101: 9463–9475
- [42] Peng XG, Schlamp MC, Kadavanich AV, Alivisatos AP (1997) Epitaxial growth of highly luminescent CdSe/CdS core/shell nanocrystals with photostability and electronic accessibility. *Journal of the American Chemical Society* 119: 7019–7029
- [43] Wei SH, Zunger A (1998) Calculated natural band offsets of all II–VI and III–V semiconductors: chemical trends and the role of cation d orbitals. *Applied Physics Letters* 72: 2011–2013
- [44] Fojtik A, Weller H, Koch U, Henglein A (1984) Photo-chemistry of colloidal metal sulfides. 8. Photophysics of extremely small CdS particles – Q-state CdS and magic agglomeration numbers. *Berichte der Bunsen-Gesellschaft für Physikalische Chemie-Physical Chemistry Chemical Physics* 88: 969–977

- [45] Spanhel L, Haase M, Weller H, Henglein A (1987) Photochemistry of colloidal semiconductors. 20. Surface modification and stability of strong luminescing CdS particles. *Journal of the American Chemical Society* 109: 5649–5655
- [46] Lianos P, Thomas JK (1986) Cadmium-sulfide of small dimensions produced in inverted micelles. *Chemical Physics Letters* 125: 299–302
- [47] Rogach A, Kershaw S, Burt M, Harrison M, Kornowski A, Eychmüller A et al (1999) Colloidally prepared HgTe nanocrystals with strong room-temperature infrared luminescence. *Advanced Materials* 11: 552–556
- [48] Harrison MT, Kershaw SV, Rogach AL, Kornowski A, Eychmüller A, Weller H (2000) Wet chemical synthesis of highly luminescent HgTe/CdS core/shell nanocrystals. *Advanced Materials* 12: 123–125
- [49] Kuno M, Higginson KA, Qadri SB, Yousuf M, Lee SH, Davis BL, Mattoussi H (2003) Molecular clusters of binary and ternary mercury chalcogenides: colloidal synthesis, characterization, and optical spectra. *Journal of Physical Chemistry B* 107: 5758–5767
- [50] LaMer VK, Dinegar RH (1950) Theory, production and mechanism of formation of mono-dispersed hydrosols. *Journal of the American Chemical Society* 72: 4847–4854
- [51] de Mello Donegá C, Liljeroth P, Vanmaekelbergh D (2005) Physicochemical evaluation of the hot-injection method, a synthesis route for monodisperse nanocrystals. *Small* 1: 1152–1162
- [52] Ostwald W (1901) *Z Physical Chemistry* 37: 385
- [53] Voorhees PW (1985) The theory of Ostwald ripening. *Journal of Statistical Physics* 38: 231–252
- [54] Reiss H (1951) The growth of uniform colloidal dispersions. *Journal of Chemical Physics* 19: 482–487
- [55] Sugimoto T (1987) Preparation of monodispersed colloidal particles. *Advances in Colloid and Interface Science* 28: 65–108
- [56] Sugimoto T, Shiba F (1999) A new approach to interfacial energy. 3. Formulation of the absolute value of the solid–liquid interfacial energy and experimental collation to silver halide systems. *Journal of Physical Chemistry B* 103: 3607–3615
- [57] Peng XG, Wickham J, Alivisatos AP (1998) Kinetics of II–VI and III–V colloidal semiconductor nanocrystal growth: “Focusing” of size distributions. *Journal of the American Chemical Society* 120: 5343–5344
- [58] Peng ZA, Peng XG (2001) Formation of high-quality CdTe, CdSe, and CdS nanocrystals using CdO as precursor. *Journal of the American Chemical Society* 123: 183–184
- [59] Qu L, Peng ZA, Peng X (2001) Alternative routes toward high quality CdSe nanocrystals. *Nano Letters* 1: 333–336
- [60] Yu W, Peng X (2002) Formation of high quality CdS and other II–VI semiconductor nanocrystals in noncoordinating solvents: tunable reactivity of monomers. *Angewandte Chemie-International Edition* 41: 2368–2371
- [61] Liu HT, Owen JS, Alivisatos AP (2007) Mechanistic study of precursor evolution in colloidal group II–VI semiconductor nanocrystal synthesis. *Journal of the American Chemical Society* 129: 305–312
- [62] Chen XB, Lou YB, Samia AC, Burda C (2003) Coherency strain effects on the optical response of core/shell heteronanostructures. *Nano Letters* 3: 799–803
- [63] Madelung O, Schulz M, Weiss H (1982) *Landolt-Börnstein: numerical data and functional relationships in science and technology, new series, group III: crystal and solid state physics, vol. III/17b*. Springer, Berlin
- [64] Singh J (1993) *Physics of semiconductors and their heterostructures*. McGraw-Hill, New York
- [65] Yu WW, Qu LH, Guo WZ, Peng XG (2003) Experimental determination of the extinction coefficient of CdTe, CdSe, and CdS nanocrystals. *Chemistry of Materials* 15: 2854–2860
- [66] Li JJ, Wang YA, Guo WZ, Keay JC, Mishima TD, Johnson MB et al (2003) Large-scale synthesis of nearly monodisperse CdSe/CdS core/shell nanocrystals using air-stable reagents via successive ion layer adsorption and reaction. *Journal of the American Chemical Society* 125: 12567–12575
- [67] Talapin DV, Rogach AL, Shevchenko EV, Kornowski A, Haase M, Weller H (2002) Dynamic distribution of growth rates within the ensembles of colloidal II–VI and III–V semiconductor nanocrystals as a factor governing their photoluminescence efficiency. *Journal of the American Chemical Society* 124: 5782–5790
- [68] Wu DG, Kordesch ME, Van Patten PG (2005) A new class of capping ligands for CdSe nanocrystal synthesis. *Chemistry of Materials* 17: 6436–6441
- [69] Yang YA, Wu H, Williams KR, Cao YC (2005) Synthesis of CdSe and CdTe nanocrystals without precursor injection. *Angewandte Chemie-International Edition* 44(41): 6712–6715
- [70] Jasieniak J, Bullen C, van Embden J, Mulvaney P (2005) Phosphine-free synthesis of CdSe nanocrystals. *Journal of Physical Chemistry B* 109: 20665–20668

- [71] Sapra S, Rogach AL, Feldmann J (2006) Phosine-free synthesis of monodisperse CdSe nanocrystals in olive oil. *Journal of Materials Chemistry* 16: 3391–3395
- [72] Pradhan N, Reifsnnyder D, Xie RG, Aldana J, Peng XG (2007) Surface ligand dynamics in growth of nanocrystals. *Journal of the American Chemical Society* 129: 9500–9509
- [73] Cao YC, Wang JH (2004) One-pot synthesis of high-quality zinc-blende CdS nanocrystals. *Journal of the American Chemical Society* 126: 14336–14337
- [74] Pradhan N, Efrima S (2003) Single-precursor, one-pot versatile synthesis under near ambient conditions of tunable, single and dual band fluorescing metal sulfide nanoparticles. *Journal of the American Chemical Society* 125: 2050–2051
- [75] Pradhan N, Katz B, Efrima S (2003) Synthesis of high-quality metal sulfide nanoparticles from alkyl xanthate single precursors in alkylamine solvents. *Journal of Physical Chemistry B* 107: 13843–13854
- [76] Joo J, Na HB, Yu T, Yu JH, Kim YW, Wu FX, Zhang JZ, Hyeon T (2003) Generalized and facile synthesis of semiconducting metal sulfide nanocrystals. *Journal of the American Chemical Society* 125: 11100–11105
- [77] Talapin DV, Haubold S, Rogach AL, Kornowski A, Haase M, Weller H (2001) A novel organometallic synthesis of highly luminescent CdTe nanocrystals. *Journal of Physical Chemistry B* 105: 2260–2263
- [78] Yu WW, Wang YA, Peng X (2003) Formation and stability of size-, shape-, and structure-controlled CdTe nanocrystals: ligand effects on monomers and nanocrystals. *Chemistry of Materials* 15(22): 4300–4308
- [79] Kloper V, Osovsky R, Kolny-Olesiak J, Sashchuk A, Lifshitz E (2007) The growth of colloidal cadmium telluride nanocrystal quantum dots in the presence of Cd-0 nanoparticles. *Journal of Physical Chemistry C* 111: 10336–10341
- [80] Li LS, Pradhan N, Wang Y, Peng X (2004) High quality ZnSe and ZnS nanocrystals formed by activating zinc carboxylate precursors. *Nano Letters* 4(11): 2261–2264
- [81] Yu JH, Joo J, Park HM, Baik SI, Kim YW, Kim SC, Hyeon T (2005) Synthesis of quantum-sized cubic ZnS nanorods by the oriented attachment mechanism. *Journal of the American Chemical Society* 127: 5662–5670
- [82] Hines MA, Guyot-Sionnest P (1998) Bright UV-blue luminescent colloidal ZnSe nanocrystals. *Journal of Physical Chemistry B* 102(19): 3655–3657
- [83] Reiss P, Quemard G, Carayon S, Bleuse J, Chandezon C, Pron A (2004) Luminescent ZnSe nanocrystals of high color purity. *Materials Chemistry and Physics* 84: 10–13
- [84] Xie R, Zhong X, Basché T (2005) Synthesis, characterization, and spectroscopy of type-II core/shell semiconductor nanocrystals with ZnTe cores. *Advanced Materials* 17: 2741–2746
- [85] Green M, Wakefield G, Dobson PJ (2003) A simple metalorganic route to organically passivated mercury telluride nanocrystals. *Journal of Materials Chemistry* 13: 1076–1078
- [86] Zhong X, Zhang Z, Liu S, Han M, Knoll W (2004) Embryonic nuclei-induced alloying process for the reproducible synthesis of blue-emitting $Zn_xCd_{1-x}Se$ nanocrystals with long-time thermal stability in size distribution and emission wavelength. *Journal of Physical Chemistry B* 108(40): 15552–15559
- [87] Steckel JS, Snee P, Coe-Sullivan S, Zimmer JR, Halpert JE, Anikeeva P et al (2006) Color-saturated green-emitting QD-LEDs. *Angewandte Chemie-International Edition* 45: 5796–5799
- [88] Protière M, Reiss P (2007) Highly luminescent $Cd_{1-x}Zn_xSe/ZnS$ core shell nanocrystals emitting in the blue-green spectral range. *Small* 3: 399–403
- [89] Zhong X, Feng Y, Knoll W, Han M (2003) Alloyed $Zn_xCd_{1-x}S$ nanocrystals with highly narrow luminescence spectral width. *Journal of the American Chemical Society* 125(44): 13559–13563
- [90] Bailey RE, Nie S (2003) Alloyed semiconductor quantum dots: tuning the optical properties without changing the particle size. *Journal of American Chemical Society* 125(23): 7100–7106
- [91] Pradhan N, Reifsnnyder D, Xie R, Aldana J, Peng X (2007) Surface ligand dynamics in growth of nanocrystals. *Journal of American Chemical Society* 129: 9500–9509
- [92] Chen HS, Lo B, Hwang JY, Chang GY, Chen CM, Tasi SJ et al (2004) Colloidal ZnSe, ZnSe/ZnS, and ZnSe/ZnSeS quantum dots synthesized from ZnO. *Journal of Physical Chemistry B* 108: 17119–17123
- [93] Bernard JE, Zunger A (1986) Optical bowing in zinc chalcogenide semiconductor alloys. *Physical Review B* 34: 5992–5995
- [94] Bernard JE, Zunger A (1987) Electronic-structure of ZnS, ZnSe, ZnTe, and their pseudobinary alloys. *Physical Review B* 36: 3199–3228
- [95] Al-Salim N, Young AG, Tilley RD, McQuillan AJ, Xia J (2007) Synthesis of CdSeS nanocrystals in coordinating and noncoordinating solvents: solvent's role in evolution of the optical and structural properties. *Chemistry of Materials* 19: 5185–5193

- [96] Furdyna JK (1988) Diluted magnetic semiconductors. *Journal of Applied Physics* 64: R29–R64
- [97] Oczkiewicz B, Twardowski A, Demianiuk M (1987) Intra-manganese absorption and luminescence in $Zn_{1-x}Mn_xSe$ semimagnetic semiconductor. *Solid State Communications* 64: 107–111
- [98] Xue J, Ye Y, Medina F, Martinez L, Lopez-Rivera SA, Giriat W (1998) Temperature evolution of the 2.1 eV band in the $Zn_{1-x}Mn_xSe$ system for low concentration. *Journal of Luminescence* 78: 173–178
- [99] Norris DJ, Yao N, Charnock FT, Kennedy TA (2001) High-quality manganese-doped ZnSe nanocrystals. *Nano Letters* 1: 3–7
- [100] Suyver JF, Wuister SF, Kelly JJ, Meijerink A (2000) Luminescence of nanocrystalline ZnSe: Mn^{2+} . *Physical Chemistry Chemical Physics* 2: 5445–5448
- [101] Norberg NS, Parks GL, Salley GM, Gamelin DR (2006) Giant excitonic Zeeman splittings in colloidal Co^{2+} -doped ZnSe quantum dots. *Journal of the American Chemical Society* 128: 13195–13203
- [102] Dance IG, Choy A, Scudder ML (1984) Syntheses, properties, and molecular and crystal-structures of $(Me_4N)_4[S_4Zn_{10}(SPh)_{16}]$ $(Me_4N)_n[Se_4Cd_{10}(SPh)_{16}]$ – molecular supertetrahedral fragments of the cubic metal chalcogenide lattice. *Journal of the American Chemical Society* 106: 6285–6295
- [103] Archer PI, Santangelo SA, Gamelin DR (2007) Inorganic cluster syntheses of TM^{2+} -doped quantum dots (CdSe, CdS, CdSe/CdS): physical property dependence on dopant locale. *Journal of the American Chemical Society* 129: 9808–9818
- [104] Erwin SC, Zu LJ, Haftel MI, Efros AL, Kennedy TA, Norris DJ (2005) Doping semiconductor nanocrystals. *Nature* 436: 91–94
- [105] Pradhan N, Peng XG (2007) Efficient and color-tunable Mn-doped ZnSe nanocrystal emitters: control of optical performance via greener synthetic chemistry. *Journal of the American Chemical Society* 129: 3339–3347
- [106] Pradhan N, Goorskey D, Thessing J, Peng XG (2005) An alternative of CdSe nanocrystal emitters: Pure and tunable impurity emissions in ZnSe nanocrystals. *Journal of the American Chemical Society* 127: 17586–17587
- [107] Pradhan N, Battaglia DM, Liu YC, Peng XG (2007) Efficient, stable, small, and water-soluble doped ZnSe nanocrystal emitters as non-cadmium biomedical labels. *Nano Letters* 7: 312–317
- [108] Green M (2002) Solution routes to III–V semiconductor quantum dots. *Current Opinion in Solid State & Materials Science* 6: 355–363
- [109] Wells RL, Gladfelter WL (1997) Pathways to nanocrystalline III–V (13–15) Compound Semiconductors. *Journal of Cluster Science* 8(2): 217–238
- [110] Mičić OI, Curtis CJ, Jones KM, Sprague JR, Nozik AJ (1994) Synthesis and characterization of InP quantum dots. *Journal of Physical Chemistry* 98: 4966–4969
- [111] Guzelian AA, Katari JEB, Kadavanich AV, Banin U, Hamad K, Juban E, Alivisatos AP, Wolters RH, Arnold CC, Heath JR (1996) Synthesis of size-selected, surface-passivated InP nanocrystals. *Journal of Physical Chemistry* 100: 7212–7219
- [112] Battaglia D, Peng XG (2002) Formation of high quality InP and InAs nanocrystals in a noncoordinating solvent. *Nano Letters* 2: 1027–1030
- [113] Xu S, Kumar S, Nann T (2006) Rapid synthesis of high-quality InP nanocrystals. *Journal of the American Chemical Society* 128: 1054–1055
- [114] Guzelian AA, Banin U, Kadavanich AV, Peng X, Alivisatos AP (1996) Colloidal chemical synthesis and characterization of InAs nanocrystal quantum dots. *Applied Physics Letters* 69: 1432–1434
- [115] Mičić OI, Sprague JR, Curtis CJ, Jones KM, Machol JL, Nozik AJ et al (1995) Synthesis and characterization of InP, GaP, and $GaInP_2$ quantum dots. *Journal of Physical Chemistry* 99: 7754–7759
- [116] Kim YH, Jun YW, Jun BH, Lee SM, Cheon JW (2002) Sterically induced shape and crystalline phase control of GaP nanocrystals. *Journal of the American Chemical Society* 124: 13656–13657
- [117] Furis M, Sahoo Y, MacRae DJ, Manciu FS, Cartwright AN, Prasad PN (2003) Surfactant-imposed interference in the optical characterization of GaP nanocrystals. *Journal of Physical Chemistry B* 107: 11622–11625
- [118] Sardar K, Dan M, Schwenzer B, Rao CNR (2005) A simple single-source precursor route to the nanostructures of AlN, GaN and InN. *Journal of Materials Chemistry* 15: 2175–2177
- [119] Green M, O'Brien P (2004) The synthesis of III–V semiconductor nanoparticles using indium and gallium diorganophosphides as single-molecular precursors. *Journal of Materials Chemistry* 14: 629–636
- [120] Sargent EH (2005) Infrared quantum dots. *Advanced Materials* 17: 515–522

- [121] Rogach AL, Eychmüller A, Hickey SG, Kershaw SV (2007) Infrared-emitting colloidal nanocrystals: synthesis, assembly, spectroscopy, and applications. *Small* 3: 536–557
- [122] Murray CB, Sun SH, Gaschler W, Doyle H, Betley TA, Kagan CR (2001) Colloidal synthesis of nanocrystals and nanocrystal superlattices. *IBM Journal of Research and Development* 45: 47–56
- [123] Sun SH, Murray CB, Weller D, Folks L, Moser A (2000) Monodisperse FePt nanoparticles and ferromagnetic FePt nanocrystal superlattices. *Science* 287: 1989–1992
- [124] Yu WW, Falkner JC, Shih BS, Colvin VL (2004) Preparation and characterization of monodisperse PbSe semiconductor nanocrystals in a noncoordinating solvent. *Chemistry of Materials* 16: 3318–3322
- [125] Hines MA, Scholes GD (2003) Colloidal PbS nanocrystals with size-tunable near-infrared emission: observation of post-synthesis self-narrowing of the particle size distribution. *Advanced Materials* 15: 1844–1849
- [126] Lu W, Fang J, Stokes KL, Lin J (2004) Shape evolution and assembly of monodisperse PbTe nanocrystals. *Journal of the American Chemical Society* 126: 11798–11799
- [127] Murphy JE, Beard MC, Norman AG, Ahrenkiel SP, Johnson JC, Yu PR et al (2006) PbTe colloidal nanocrystals: synthesis, characterization, and multiple exciton generation. *Journal of the American Chemical Society* 128: 3241–3247
- [128] Houtepen AJ, Koole R, Vanmaekelbergh DL, Meeldijk J, Hickey SG (2006) The hidden role of acetate in the PbSe nanocrystal synthesis. *Journal of the American Chemical Society* 128: 6792–6793
- [129] Wehrenberg BL, Wang CJ, Guyot-Sionnest P (2002) Interband and intraband optical studies of PbSe colloidal quantum dots. *Journal of Physical Chemistry B* 106: 10634–10640
- [130] Steckel JS, Coe-Sullivan S, Bulovic V, Bawendi MG (2003) 1.3 μm to 1.55 μm tunable electroluminescence from PbSe quantum dots embedded within an organic device. *Advanced Materials* 15 (21): 1862–1866
- [131] Pietryga JM, Schaller RD, Werder D, Stewart MH, Klimov VI, Hollingsworth JA (2004) Pushing the band gap envelope: mid-infrared emitting colloidal PbSe quantum dots. *Journal of the American Chemical Society* 126: 11752–11753
- [132] Baek IC, Il Seok S, Pramanik NC, Jana S, Lim MA, Ahn BY et al (2007) Ligand-dependent particle size control of PbSe quantum dots. *Journal of Colloid and Interface Science* 310: 163–166
- [133] Sashchiuk A, Amirav L, Bashouti M, Krueger M, Sivan U, Lifshitz E (2004) PbSe nanocrystal assemblies: synthesis and structural, optical, and electrical characterization. *Nano Letters* 4: 159–165
- [134] Nairn JJ, Shapiro PJ, Twamley B, Pounds T, von Wandruszka R, Fletcher TR et al (2006) Preparation of ultrafine chalcopyrite nanoparticles via the photochemical decomposition of molecular single-source precursors. *Nano Letters* 6: 1218–1223
- [135] Czekelius C, Hilgendorff M, Spanhel L, Bedja I, Lerch M, Müller G et al (1999) A simple colloidal route to nanocrystalline ZnO/CuInS₂ bilayers. *Advanced Materials* 11: 643–646
- [136] Banger KK, Jin MHC, Harris JD, Fanwick PE, Hepp AF (2003) A new facile route for the preparation of single-source precursors for bulk, thin-film, and nanocrystalline I–III–VI semiconductors. *Inorganic Chemistry* 42: 7713–7715
- [137] Gurinowich LI, Gurin VS, Ivanov VA, Molochko AP, Solovei NP (1998) Optical properties of CuInS₂ nanoparticles in the region of the fundamental absorption edge. *Journal of Applied Spectroscopy* 63(3): 401–407
- [138] Wakita K, Fujita F, Yamamoto N (2001) Photoluminescence excitation spectra of CuInS₂ crystals. *Journal of Applied Physics* 90: 1292–1296
- [139] Castro SL, Bailey SG, Raffaele RP, Banger KK, Hepp AF (2004) Synthesis and characterization of colloidal CuInS₂ nanoparticles from a molecular single-source precursor. *Journal of Physical Chemistry B* 108: 12429–12435
- [140] Castro SL, Bailey SG, Raffaele RP, Banger KK, Hepp AF (2003) Nanocrystalline chalcopyrite materials (CuInS₂ and CuInSe₂) via low-temperature pyrolysis of molecular single-source precursors. *Chemistry of Materials* 15: 3142–3147
- [141] Choi SH, Kim EG, Hyeon T (2006) One-pot synthesis of copper-indium sulfide nanocrystal heterostructures with acorn, bottle, and larva shapes. *Journal of the American Chemical Society* 128: 2520–2521
- [142] Nakamura H, Kato W, Uehara M, Nose K, Omata T, Otsuka-Yao-Matsuo S et al (2006) Tunable photoluminescence wavelength of chalcopyrite CuInS₂-based semiconductor nanocrystals synthesized in a colloidal system. *Chemistry of Materials* 18: 3330–3335
- [143] Torimoto T, Adachi T, Okazaki K, Sakuraoka M, Shibayama T, Ohtani B et al (2007) Facile synthesis of ZnS-AgInS₂ solid solution nanoparticles for a color-adjustable luminophore. *Journal of the American Chemical Society* 129: 12388–12389

- [144] Malik MA, O'Brien P, Revaprasadu N (1999) A novel route for the preparation of CuSe and CuInSe₂ nanoparticles. *Advanced Materials* 11: 1441–1444
- [145] Zhong HZ, Li YC, Ye MF, Zhu ZZ, Zhou Y, Yang CH et al (2007) A facile route to synthesize chalcopyrite CuInSe₂ nanocrystals in non-coordinating solvent. *Nanotechnology* 18: 025602
- [146] English DS, Pell LE, Yu ZH, Barbara PF, Korgel BA (2002) Size tunable visible luminescence from individual organic monolayer stabilized silicon nanocrystal quantum dots. *Nano Letters* 2: 681–685
- [147] Holmes JD, Ziegler KJ, Doty RC, Pell LE, Johnston KP, Korgel BA (2001) Highly luminescent silicon nanocrystals with discrete optical transitions. *Journal of the American Chemical Society* 123: 3743–3748
- [148] Hanrath T, Korgel BA (2003) Supercritical fluid–liquid–solid (SFLS) synthesis of Si and Ge nanowires seeded by colloidal metal nanocrystals. *Advanced Materials* 15: 437–440
- [149] Pell LE, Schrickler AD, Mikulec FV, Korgel BA (2004) Synthesis of amorphous silicon colloids by trisilane thermolysis in high temperature supercritical solvents. *Langmuir* 20: 6546–6548
- [150] Tilley RD, Warner JH, Yamamoto K, Matsui I, Fujimori H (2005) Micro-emulsion synthesis of monodisperse surface stabilized silicon nanocrystals. *Chemical Communications* 1833–1835
- [151] Warner JH, Hoshino A, Yamamoto K, Tilley RD (2005) Water-soluble photoluminescent silicon quantum dots. *Angewandte Chemie-International Edition* 44: 4550–4554
- [152] Taylor BR, Kaulzarich SM, Delgado GR, Lee HWH (1999) Solution synthesis and characterization of quantum confined Ge nanoparticles. *Chemistry of Materials* 11: 2493–2500
- [153] Yang CS, Bley RA, Kaulzarich SM, Lee HWH, Delgado GR (1999) Synthesis of alkyl-terminated silicon nanoclusters by a solution route. *Journal of the American Chemical Society* 121: 5191–5195
- [154] Heath JR, Shiang JJ, Alivisatos AP (1994) Germanium quantum dots – optical properties and synthesis. *Journal of Chemical Physics* 101: 1607–1615
- [155] Mokari T, Banin U (2003) Synthesis and properties of CdSe/ZnS core/shell nanorods. *Chemistry of Materials* 15: 3955–3960
- [156] Kudera S, Zanella M, Giannini C, Rizzo A, Li YQ, Gigli G, Cingolani R, Ciccarella G, Spahl W, Parak WJ, Manna L (2007) Sequential growth of magic-size CdSe nanocrystals. *Advanced Materials* 19: 548–552
- [157] Jun S, Jang E (2005) Interfused semiconductor nanocrystals: brilliant blue photoluminescence and electroluminescence. *Chemical Communications* 36: 4616–4618
- [158] Wang S, Jarrett BR, Kaulzarich SM, Louie AY (2007) Core/shell quantum dots with high relaxivity and photoluminescence for multimodality imaging. *Journal of the American Chemical Society* 129: 3848–3856
- [159] Revaprasadu N, Malik MA, O'Brien P, Wakefield G (1999) A simple route to synthesize nanodimensional CdSe–CdS core-shell structures from single molecule precursors. *Chemical Communications* 1573–1574
- [160] Malik MA, O'Brien P, Revaprasadu N (2002) A simple route to the synthesis of core/shell nanoparticles of chalcogenides. *Chemistry of Materials* 14: 2004–2010
- [161] Mekis I, Talapin DV, Kornowski A, Haase M, Weller H (2003) One-pot synthesis of highly luminescent CdSe/CdS core-shell nanocrystals via organometallic and “greener” chemical approaches. *Journal of Physical Chemistry B* 107: 7454–7462
- [162] Pan DC, Wang Q, Jiang SC, Ji XL, An LJ (2005) Synthesis of extremely small CdSe and highly luminescent CdSe/CdS core-shell nanocrystals via a novel two-phase thermal approach. *Advanced Materials* 17: 176–179
- [163] Danek M, Jensen KF, Murray CB, Bawendi MG (1996) Synthesis of luminescent thin-film CdSe/ZnSe quantum dot composites using CdSe quantum dots passivated with an overlayer of ZnSe. *Chemistry of Materials* 8: 173–180
- [164] Reiss P, Bleuse J, Pron A (2002) Highly luminescent CdSe/ZnSe core/shell nanocrystals of low size dispersion. *Nano Letters* 2: 781–784
- [165] Lee YJ, Kim TG, Sung YM (2006) Lattice distortion and luminescence of CdSe/ZnSe nanocrystals. *Nanotechnology* 17: 3539–3542
- [166] Sung YM, Park KS, Lee YJ, Kim TG (2007) Ripening kinetics of CdSe/ZnSe core/shell nanocrystals. *Journal of Physical Chemistry C* 111: 1239–1242
- [167] Steckel JS, Zimmer JP, Coe-Sullivan S, Stott NE, Bulovic V, Bawendi MG (2004) Blue luminescence from (CdS)ZnS core-shell nanocrystals. *Angewandte Chemie-International Edition* 43: 2154–2158
- [168] Protière M, Reiss P (2006) Facile synthesis of monodisperse ZnS capped CdS nanocrystals exhibiting efficient blue emission. *Nanoscale Research Letters* 1: 62–67

- [169] Yang YA, Chen O, Angerhofer A, Cao YC (2006) Radial-position-controlled doping in CdS/ZnS core/shell nanocrystals. *Journal of the American Chemical Society* 128: 12428–12429
- [170] Lomascolo M, Creti A, Leo G, Vasanelli L, Manna L (2003) Exciton relaxation processes in colloidal core/shell ZnSe/ZnS nanocrystals. *Applied Physics Letters* 82: 418–420
- [171] Chen HS, Lo B, Hwang JY, Chang GY, Chen CM, Tasi SJ et al (2004) Colloidal ZnSe, ZnSe/ZnS, and ZnSe/ZnSeS quantum dots synthesized from ZnO. *Journal of Physical Chemistry B* 108: 17119–17123
- [172] Tsay JM, Pflughoeft M, Bentolila LA, Weiss S (2004) Hybrid approach to the synthesis of highly luminescent CdTe/ZnS and CdHgTe/ZnS nanocrystals. *Journal of the American Chemical Society* 126: 1926–1927
- [173] Haubold S, Haase M, Kornowski A, Weller H (2001) Strongly luminescent InP/ZnS core-shell nanoparticles. *Chem Phys Chem* 2: 331–334
- [174] Micić OI, Smith BB, Nozik AJ (2000) Core-shell quantum dots of lattice-matched ZnCdSe₂ shells on InP cores: experiment and theory. *Journal of Physical Chemistry B* 104: 12149–12156
- [175] Cao YW, Banin U (1999) Synthesis and characterization of InAs/InP and InAs/CdSe core/shell nanocrystals. *Angewandte Chemie-International Edition* 38: 3692–3694
- [176] Cao YW, Banin U (2000) Growth and properties of semiconductor core/shell nanocrystals with InAs cores. *Journal of the American Chemical Society* 122: 9692–9702
- [177] Kim SW, Zimmer JP, Ohnishi S, Tracy JB, Frangioni JV, Bawendi MG (2005) Engineering InAs_xP_{1-x}/InP/ZnSe III–V alloyed core/shell quantum dots for the near-infrared. *Journal of the American Chemical Society* 127: 10526–10532
- [178] Sashchiuk A, Langof L, Chaim R, Lifshitz E (2002) Synthesis and characterization of PbSe and PbSe/PbS core-shell colloidal nanocrystals. *Journal of Crystal Growth* 240: 431–438
- [179] Brumer M, Kigel A, Amirav L, Sashchiuk A, Solomesch O, Tessler N et al (2005) PbSe/PbS and PbSe/PbSe_xS_{1-x} core/shell nanoparticles. *Advanced Functional Materials* 15: 1111–1116
- [180] Lifshitz E, Brumer M, Kigel A, Sashchiuk A, Bashouti M, Sirota M et al (2006) Stable PbSe/PbS and PbSe/PbSe_xS_{1-x} core-shell nanocrystal quantum dots and their applications. *Journal of Physical Chemistry B* 110: 25356–25365
- [181] Xu J, Cui DH, Zhu T, Paradee G, Liang ZQ, Wang Q et al (2006) Synthesis and surface modification of PbSe/PbS core-shell nanocrystals for potential device applications. *Nanotechnology* 17: 5428–5434
- [182] Kim S, Fisher B, Eisler HJ, Bawendi M (2003) Type-II quantum dots: CdTe/CdSe(core/shell) and CdSe/ZnTe(core/shell) heterostructures. *Journal of the American Chemical Society* 125: 11466–11467
- [183] Yu K, Zaman B, Romanova S, Wang DS, Ripmeester JA (2005) Sequential synthesis of type II colloidal CdTe/CdSe core-shell nanocrystals. *Small* 1: 332–338
- [184] Chen CY, Cheng CT, Yu JK, Pu SC, Cheng YM, Chou PT et al (2004) Spectroscopy and femtosecond dynamics of type-II CdSe/ZnTe core-shell semiconductor synthesized via the CdO precursor. *Journal of Physical Chemistry B* 108: 10687–10691
- [185] Balet LP, Ivanov SA, Piryatinski A, Achermann M, Klimov VI (2004) Inverted core/shell nanocrystals continuously tunable between type-I and type-II localization regimes. *Nano Letters* 4: 1485–1488
- [186] Zhong XH, Xie RG, Zhang Y, Basché T, Knoll W (2005) High-quality violet- to red-emitting ZnSe/CdSe core/shell nanocrystals. *Chemistry of Materials* 17: 4038–4042
- [187] Xie RG, Zhong XH, Basché T (2005) Synthesis, characterization, and spectroscopy of type-II core/shell semiconductor nanocrystals with ZnTe cores. *Advanced Materials* 17: 2741–2744
- [188] Milliron DJ, Hughes SM, Cui Y, Manna L, Li JB, Wang LW, Alivisatos AP (2004) Colloidal nanocrystal heterostructures with linear and branched topology. *Nature* 430: 190–195
- [189] Xie RG, Kolb U, Basché T (2006) Design and synthesis of colloidal nanocrystal heterostructures with tetrapod morphology. *Small* 2: 1454–1457
- [190] Burda C, Chen XB, Narayanan R, El-Sayed MA (2005) Chemistry and properties of nanocrystals of different shapes. *Chemical Reviews* 105: 1025–1102
- [191] Kumar S, Nann T (2006) Shape control of II–VI semiconductor nanomaterials. *Small* 2: 316–329
- [192] Carbone L, Nobile C, De Giorgi M, Sala FD, Morello G, Pompa P et al (2007) Synthesis and micrometer-scale assembly of colloidal CdSe/CdS nanorods prepared by a seeded growth approach. *Nano Letters* 7: 2942–2950
- [193] Talapin DV, Nelson JH, Shevchenko EV, Aloni S, Sadtler B, Alivisatos AP (2007) Seeded growth of highly luminescent CdSe/CdS nanoheterostructures with rod and tetrapod morphologies. *Nano Letters* 7: 2951–2959